[American Journal of Science, Vol. 303, November, 2003, P. 817–855]

EROSION OF AN ANCIENT MOUNTAIN RANGE, THE GREAT SMOKY MOUNTAINS, NORTH CAROLINA AND TENNESSEE

MATMON, A.*†, BIERMAN, P. R.*, LARSEN, J.*, SOUTHWORTH, S.**, PAVICH, M.**, FINKEL, R.***, and CAFFEE, M.***††

ABSTRACT. Analysis of ^{10}Be and ^{26}Al in bedrock (n=10), colluvium (n=5 including grain size splits), and alluvial sediments (n=59 including grain size splits), coupled with field observations and GIS analysis, suggest that erosion rates in the Great Smoky Mountains are controlled by subsurface bedrock erosion and diffusive slope processes. The results indicate rapid alluvial transport, minimal alluvial storage, and suggest that most of the cosmogenic nuclide inventory in sediments is accumulated while they are eroding from bedrock and traveling down hill slopes.

Spatially homogeneous erosion rates of 25 - 30 mm Ky^{-1} are calculated throughout the Great Smoky Mountains using measured concentrations of cosmogenic ^{10}Be and ^{26}Al in quartz separated from alluvial sediment. ^{10}Be and ^{26}Al concentrations in sediments collected from headwater tributaries that have no upstream samples (n=18) are consistent with an average erosion rate of 28 ± 8 mm Ky^{-1}, similar to that of the outlet rivers (n=16, 24 ± 6 mm Ky^{-1}), which carry most of the sediment out of the mountain range.

Grain-size-specific analysis of 6 alluvial sediment samples shows higher nuclide concentrations in smaller grain sizes than in larger ones. The difference in concentrations arises from the large elevation distribution of the source of the smaller grains compared with the narrow and relatively low source elevation of the large grains. Large sandstone clasts disaggregate into sand-size grains rapidly during weathering and downslope transport; thus, only clasts from the lower parts of slopes reach the streams. ^{26}Al/^{10}Be ratios do not suggest significant burial periods for our samples. However, alluvial samples have lower ^{26}Al/^{10}Be ratios than bedrock and colluvial samples, a trend consistent with a longer integrated cosmic ray exposure history that includes periods of burial during down-slope transport.

The results confirm some of the basic ideas embedded in Davis' *geographic cycle* model, such as the reduction of relief through slope processes, and of Hack's *dynamic equilibrium* model such as the similarity of erosion rates across different lithologies. Comparing cosmogenic nuclide data with other measured and calculated erosion rates for the Appalachians, we conclude that rates of erosion, integrated over varying time periods from decades to a hundred million years are similar, the result of equilibrium between erosion and isostatic uplift in the southern Appalachian Mountains.

INTRODUCTION

The persistence of mountain ranges over hundreds of millions of years is a major geologic paradox. Many models (Ahnert, 1970; Pinet and Souriau, 1988; Harrison, 1994; Tucker and Slingerland, 1994; Beaumont and others, 2000) require that mountain ranges should disappear in 10^7 to 10^8 years, suggesting that we do not yet have an adequate understanding to explain the long-term evolution of ancient topographic features. The Appalachian Mountains (fig. 1), one of the largest and most studied ancient orogenic belts, were built by a series of collisional events in the Paleozoic and an extensional event in the Late Triassic related to the opening of the Atlantic Ocean (Friedman and Sanders, 1982; Blackmer and others, 1994; Boettcher and Milliken, 1994; Pazzaglia and Brandon, 1996). Thus, the Appalachians Mountains

*Geology Department, University of Vermont, Burlington, Vermont 05405
**United States Geological Survey, Reston, Virginia 20192
***Lawrence Livermore National Laboratory, Livermore, California 94550
†Current address: US Geological Survey, 345 Middlefield Rd., MS#977, Menlo Park, California 94025; amatmon@usgs.gov
††Current address: Prime Laboratory, Physics Department, Purdue University, West Lafayette, Indiana 47907

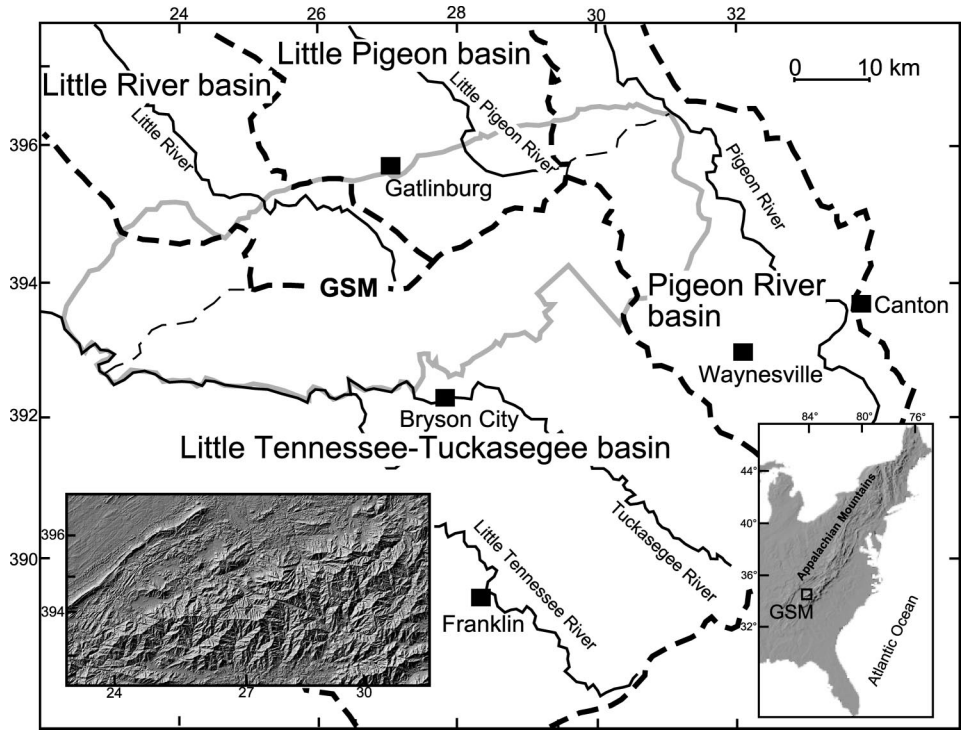

Fig. 1. Location map (UTM grid). Gray line – boundary of Great Smoky Mountains National Park. Thick dashed line – divides between major river systems in the region. Thin dashed line – GSM main drainage divide. Right inset: location of Great Smoky Mountains (GSM) in the eastern United States (DEM source http://fermi.jhuapl.edu/states/us/us_map.html accessed August 2002). Left inset: Shaded relief image of the Great Smoky Mountains (UTM grid, source: USGS).

are long-lived features providing an ideal setting to study post-orogenic denudation rates and processes. Understanding the survival of these and other ancient mountain ranges requires quantitative measurements of the rate at which they erode over time and space.

A variety of studies have investigated Appalachian landscapes and structures (Hack, 1982), as well as the stratigraphy of related coastal plain sediments and offshore basins. The initial topography of the Appalachians, following the Alleghenian orogeny, was likely similar to that of Cenozoic mountain-belts with an average elevation of 3000 to 4000 meters (Slingerland and Furlong, 1989). Rapid erosion during the Permian and Triassic removed much of this mass (and topography) and deposited it into west-lying basins.

An increase in topography and relief occurred during the Jurassic rifting and opening of the Atlantic Ocean (Judson, 1975). The eastern offshore basins that formed at that time contain a ~7 kilometer thick sedimentary sequence of detritus shed from the Appalachian Mountains since the onset of Atlantic rifting, ~180 Ma (Poag and Sevon, 1989). These sediments indicate rapid accumulation during the Jurassic, following the initial stages of seafloor spreading in the Atlantic, several periods of rapid accumulation during the Cretaceous, and deposition of a large pulse of sediment during the Miocene (Pazzaglia and Gardner, 2000). Variations in sediment accumulation rates in the offshore basins have been attributed to increases and decreases in erosion rates in the Appalachian Mountains (Poag and Sevon, 1989). Increased erosion rates during the Miocene are supported by fission track dating

(Roden and Miller, 1989; Boettcher and Milliken, 1994). However, the driving forces for erosion rate and sediment flux changes are poorly constrained and are explained by different mechanisms ranging from tectonic (Hack, 1982) to climatic (Barron, 1989).

The topography of the Appalachian Mountains is gentle compared with tectonically active mountain belts and only few summits are higher than 2000 meters above sea level. However, crustal thickness underneath the Appalachian Mountains is relatively thick (40 - 50 km; Hutchinson and others, 1983; Iverson and Smithson, 1983) and is more typical of higher mountains. The thick crust of the Appalachian Mountains represents a mountain root that may be partly the result of late Paleozoic crustal loading (Hutchinson and others, 1983) and which did not extend or thinned since its formation.

Cosmogenic nuclide analysis has proven to be a useful tool for understanding geologic rates of surface change and bedrock erosion because the penetration depth of cosmic rays buffers the impact of both human-induced and naturally-forced episodic erosion (Lal, 1991; Bierman, 1994; Bierman and Steig, 1996). The Great Smoky Mountains (fig. 1), a well-studied, moderate-size, quartz-rich range in the southern Appalachian Mountains, provide a good setting in which to employ cosmogenic nuclides as a monitor of denudation on the 10^5 year time scale. The height of the Great Smoky Mountains, their remoteness, and preservation by the National Park that includes them, make this range a good site for investigating long-term erosion rates and a good proxy for the natural erosion pattern in the unglaciated southern Appalachian Mountains. The existing broad geological and structural database enables us to test whether differences in erosion relate to geology and structure.

This study represents a systematic application of cosmogenic nuclide analysis to the drainage basins of an old mountain range in a humid region. Our sampling strategy was designed to test physical factors that presumably control erosion in the Great Smoky Mountains and, thus, to test hypotheses such as the *Dynamic Equilibrium* model (Hack, 1960) and the *Geographic Cycle* (Davis, 1899). These two contrasting models were tested by determining whether the mountain range is eroding uniformly or whether relief is increasing because erosion rates differ spatially. Sampling also helped to assess whether erosion rates are independent of lithology as suggested by the *Dynamic Equilibrium* model (Hack, 1960). The methods proposed by Bierman and Steig (1996), Granger and others (1996), and Brown and others (1995) for estimating basin-scale erosion rates were tested quantitatively by sampling three drainage systems in detail and by comparing cosmogenic-based sediment yield estimates with mass balance calculations.

We measured cosmogenic nuclide concentrations in alluvial sediments, bedrock, and colluvium and compared the results with other short and long-term estimates of erosion rates. The spatial distribution of our samples enabled us to assess the influence of lithology, climate and topographic characteristics on the rate of denudation. We determined the role of grain size on cosmogenic nuclide concentrations and show that fine sand appears to represent the average exposure history of sediments in each sampled basin. Our results suggest that slope processes control exposure histories. The results also suggest similarity between short-term rates of erosion and long-term rates of rock uplift in the southern Appalachian Mountains.

This study expands upon earlier work (Matmon and others, 2003) and includes nearly three times more data. In this study, we emphasize the distribution of erosion rates throughout the Great Smoky Mountains as well as the correlation of erosion rates with basin scale physical parameters including slope, relief, and precipitation.

BACKGROUND

The Great Smoky Mountains

The Great Smoky Mountains, located on the border between North Carolina and Tennessee, are the highest range in the southern Appalachian Mountains, rising more

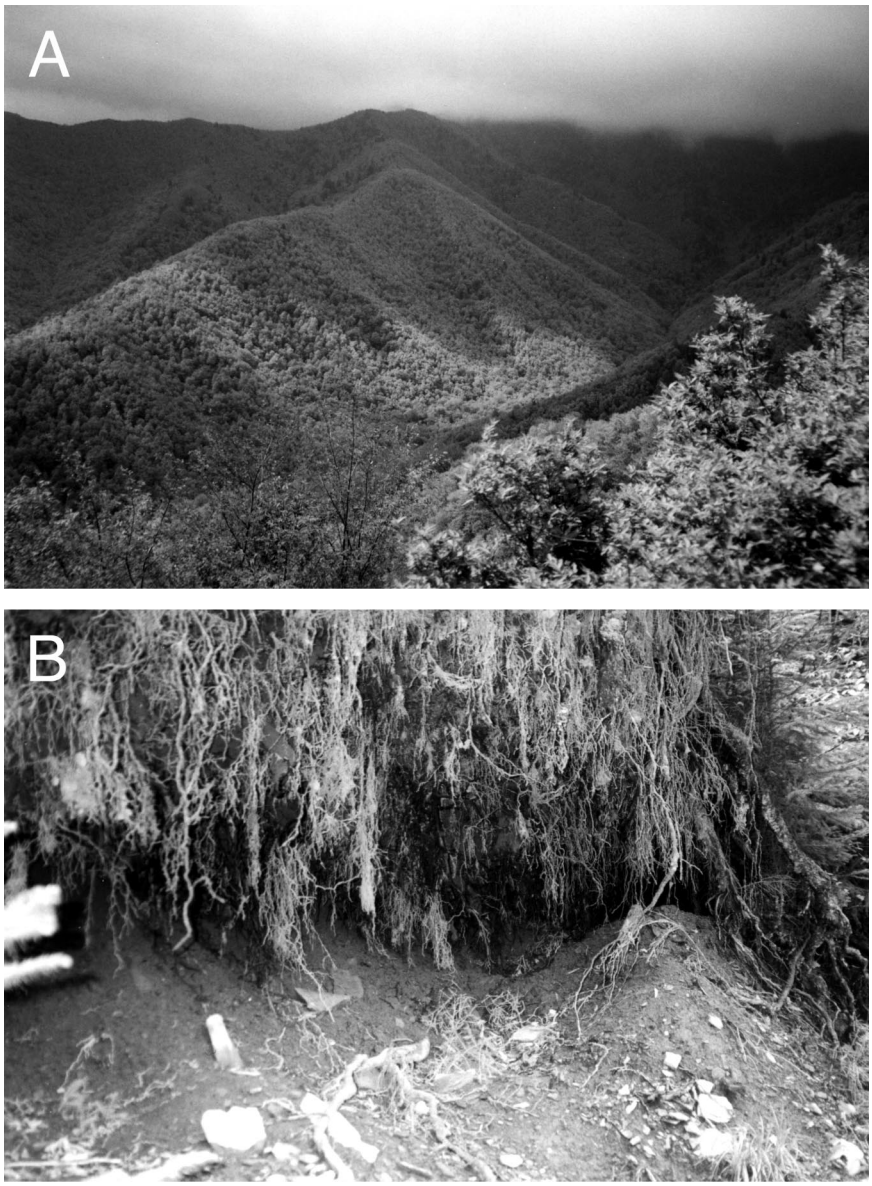

Fig. 2. (A) Upstream view of the Big Creek drainage system. Ridge tops are flat and are connected to the deeply incised rivers by steep slopes. Ridge tops and slopes are heavily vegetated. (B) Tree throw exposes sandy soil along the main Great Smoky Mountain water divide (beside the Appalachian Trail). Sand mound below roots is about 50 cm high.

than 1500 meters above the adjacent Little Tennessee River and French Broad River valleys (fig. 1). Relief in the Great Smoky Mountains is significant. Steep slopes connect flat ridge crests with deeply incised river valleys (fig. 2A). Slopes and mountain crests are soil-covered and heavily vegetated (fig. 2E). Mean annual rainfall ranges from 140 to 230 centimeters, depending on elevation (http://www.nps.gov/grsm/gsmsite/natureinfo.html; 5/02). Only minor gullying and storm-related landslide scars are

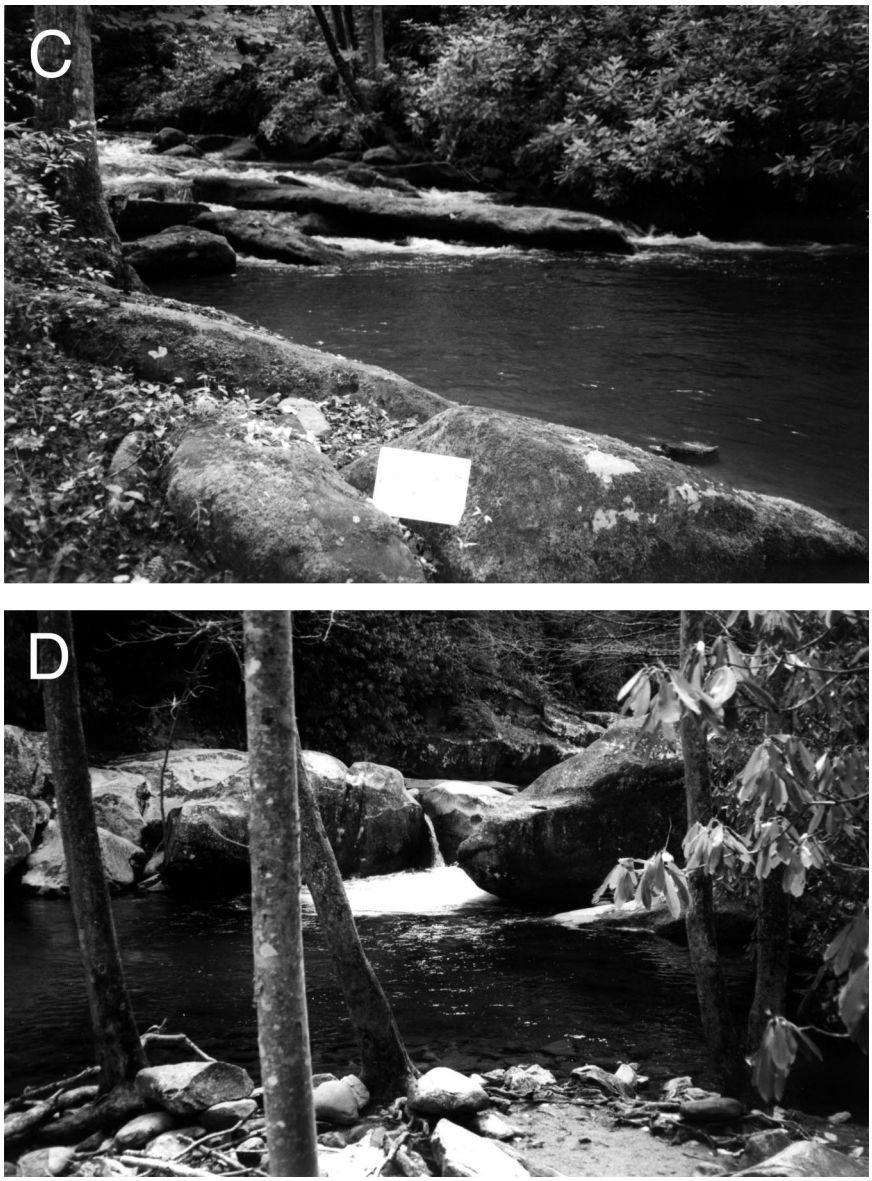

Fig. 2. (continued) (C) Typical pool in Great Smoky Mountain stream (Abrams Creek, sample GSAC-1). Alluvial sediments from pools like this were sampled. White board in foreground is 30 cm wide. (D) Sediment was also sampled from sand bars, such as the 2 meter wide bar in the foreground (Big Creek, sample GSBC-1).

evident on hill slopes and there is abundant evidence for the operation of diffusive processes, such as tree throw (fig. 2B), soil creep, and bioturbation.

The geology of the Great Smoky Mountains has been studied for over 100 years (Keith, 1895; Glenn, 1926; Hamilton, 1961; Hadley and Goldsmith, 1963; King, 1964; Southworth, 1995, 2001; Southworth and others, 1999; Schultz and Southworth, 1999; Schultz and others, 2000; Naeser and others, 1999, 2001). The constructional history,

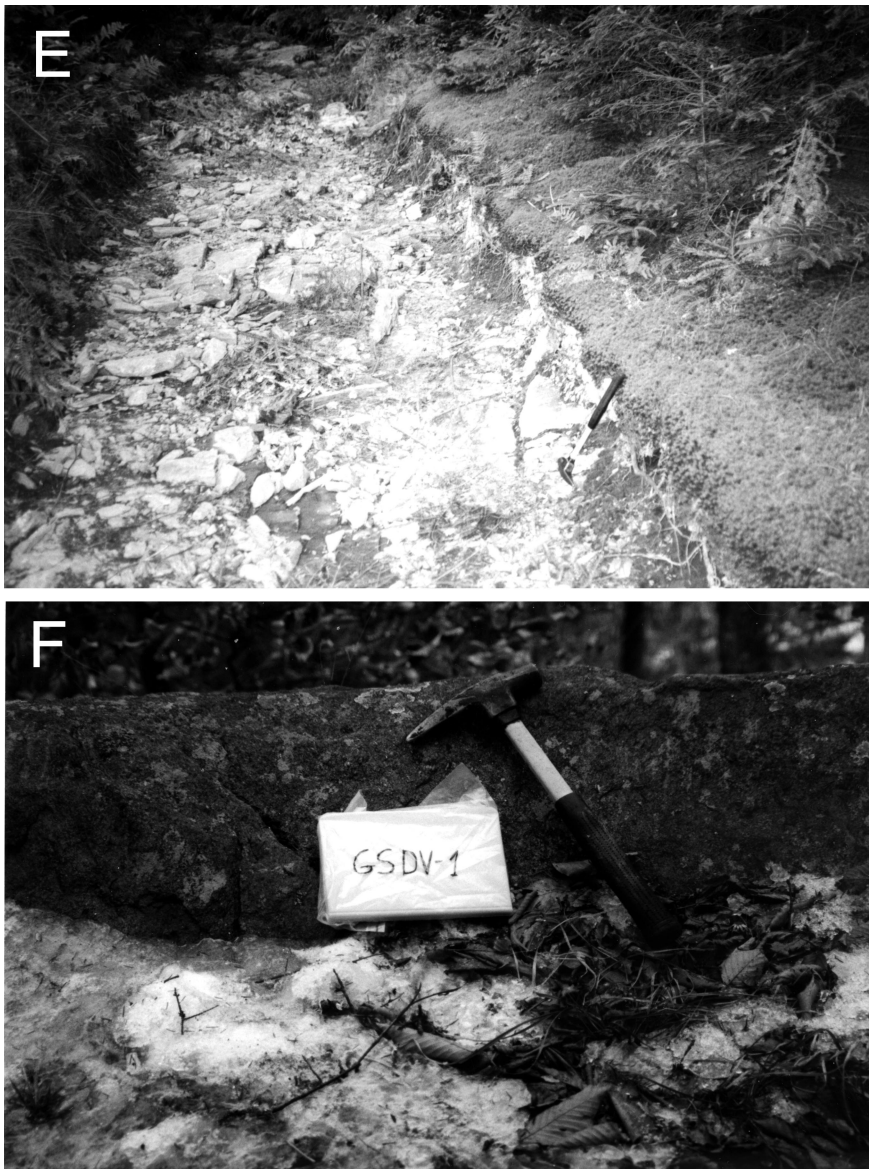

Fig. 2. (continued) (E) The soil mantle covers the entire slope environment, from the alluvial channel to the ridge tops. Soil section in photo is exposed along the Great Smoky Mountain main drainage divide due to compaction and erosion along the Appalachian Trail. Soil at top of ridge is 20-30 cm deep. Rock pick for scale. (F) Bedrock outcrop of Thunderhead Formation sandstone along the Great Smoky Mountain main drainage divide (1.6 km northeast of Newfound Gap, sample GSDV-1). The outcrops along the divide rise 1-4 meters above their surroundings. Rock pick for scale.

structure, and lithology of the range are fairly well understood. The Great Smoky Mountains are built of medium grade, metamorphosed sedimentary rocks of Neoproterozoic to early Cambrian age with isolated areas of Mesoproterozoic gneiss (King and others, 1968). These rocks were transported perhaps 100 kilometers westward to their current location above the Great Smoky thrust fault about 280 million years ago during

Fig. 2. (continued) (G) The Cosby Fan area. The surface of the fan is seen in the foreground dissected by active channels. The Great Smoky Mountain northern front is in the background. Samples GSCS-1 and GSCS-2 were collected on this fan. Ridge crest is about 10 km long.

the continental collision of the Alleghenian orogeny (King and others, 1968). However, the spatial and temporal patterns by which the Great Smoky Mountains specifically, and the southern Appalachians, in general, have and are being eroded is not as well understood despite numerous geomorphic studies, the first of which was completed over 100 years ago (for example Davis, 1889, 1899; Hack, 1960, 1979; Mills and others, 1987; Poag and Sevon, 1989; Mills, 2000a, 2000b).

Physiography.—Our study area is within the Great Smoky Mountains National Park (fig. 1). Topographically, the Great Smoky Mountains are an isolated upland bounded by the Little Tennessee River and Tuckasegee River to the south and west, and the Pigeon River to the east. These rivers originate southeast of the Great Smoky Mountains, and they flow to join the Ohio and Mississippi Rivers emptying into the Gulf of Mexico. North of the Great Smoky Mountains, limestone and dolomite underlie the Tennessee Valley, in stark contrast to the siliceous rocks of the Great Smoky Mountains. Four main river systems drain the Great Smoky Mountains National Park (fig. 1). The Pigeon River-Little Tennessee/Tuckasegee River divide trends northerly along the Balsam Mountains and transects the strike of the regional geology. The drainage divide between the Little Tennessee-Tuckasegee Rivers and Little Pigeon River-Little River runs along the summit of the Great Smoky Mountains and follows the northeast strike of the regional geology.

Structural and bedrock control of drainage systems.—Most drainages in the Great Smoky Mountains flow on bedrock but only a few flow parallel to the bedrock structure. Parts of Abrams Creek, Twenty-Mile Creek, Eagle Creek, Hazel Creek, Forney Creek, Raven Fork, and the Straight Fork flow parallel to the strike of bedding and the penetrative foliation in folded rocks (fig. 3). Only parts of the Oconaluftee River and the Straight Fork flow parallel to interpreted and known faults such as the Oconaluftee Fault (fig. 3).

Alluvial terraces are restricted to the perimeters of the mountain range and are found along the Tuckasegee River south of the Great Smoky Mountains and along the

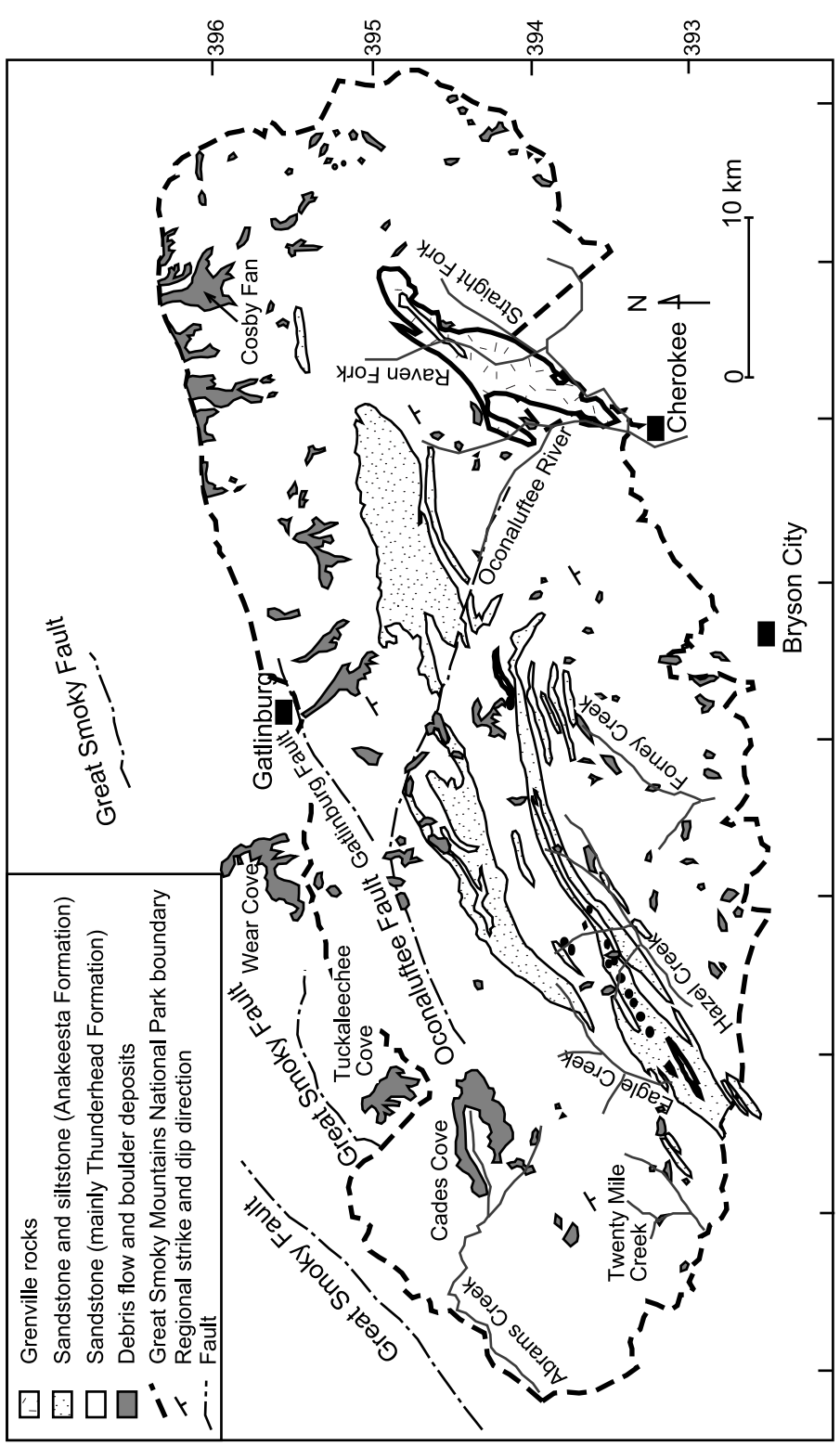

Fig. 3. Geologic map of the Great Smoky Mountains (UTM grid). Only main lithologies are shown. Quartz-bearing rocks underlie most of the range. Geology after Hamilton, 1961; Hadley and Goldsmith, 1963; King, 1964; King and others, 1968.

lower reaches of the Raven Fork and Oconaluftee River in the Cherokee area of North Carolina, where the bedrock is granitic gneiss. Elsewhere, well-developed terraces are found where drainages cross carbonate rock and fine-grained metasiltstone. There are only few sites of significant alluvial storage within the boundaries of the Great Smoky Mountains National Park; thus, all but two of our samples are unaffected by long-term, large-scale sediment storage.

Bedrock and surface morphology.—The Great Smoky Mountains are mostly underlain by resistant, quartz-rich, metamorphosed conglomeratic sandstone (Thunderhead Sandstone) and slate (Anakeesta Formation) of the Great Smoky Group (King, 1964, fig. 3). The Great Smoky Mountain drainage divide is subparallel to the strike of the metasandstone units. In the eastern part of the Great Smoky Mountains, the northwest side of the divide is characterized by massive southeast-dipping beds that form cliffs. These massive beds of metasandstone taper to the southwest where the cliffs and outcrop diminish. The distribution of large, inactive fan deposits corresponds with the north-facing massive metasandstone cliffs. These bouldery fan deposits are deeply incised by the present drainage system. The ages of the coarse fan deposits are unknown. A premier example is the Cosby Fan in the northeast part of the park (figs. 2G and 3), which consists of coarse boulders of metasandstone in a fine grain matrix (Schultz and Southworth, 1999).

The southeast side of most of the divide is either a dip slope or folded units with few outcrops. Anakeesta Formation slate underlies a broad area of the divide in the eastern part of the Great Smoky Mountains (fig. 3). This area is characterized by craggy topography with cliffs due in part to historical, storm-related debris flows (Schultz and others, 2000). Mesoproterozoic granitic gneiss is exposed in antiforms in the south-southeastern part of the Great Smoky Mountains.

Erosion of tectonic structures has created karst valleys. Extending across the foothills of the Great Smoky Mountains are karst valleys of Ordovician limestone preserved in the tectonic windows of the Great Smoky thrust fault (fig 3). Some of these valleys such as Cades Cove, Tuckaleechee Cove, and Wear Cove preserve fluvial terrace deposits and fan deposits of colluvium derived from the clastic rocks above the thrust fault high on the slopes (Schultz and Southworth, 1999).

Surface processes.—Our field observations suggest the pattern and process by which mass is removed from the Great Smoky Mountains. Bedrock outcrops on slopes and on ridge tops are rare and appear most commonly where the Thunderhead Formation sandstone underlies the landscape. Slope soil profiles exhibit well-defined horizons. There is very little evidence of soil stripping in the form of gullies and rills. The effect of raindrop impact is minimized by the dense canopy cover and the high organic matter content of the surface soils allows water to infiltrate very quickly, thus limiting overland flow even during very high intensity rainfall (Carson and Kirkby, 1972, p. 64). Scree slopes and coarse colluvial aprons on and below slopes are not abundant. However, where such mappable deposits exist, they originate in the Thunderhead Formation sandstone.

Within the mountain range, significant storage of sediment is restricted to the slopes rather than to the stream channels. Alluvial storage in fans, flood plains, and terraces is limited. Despite the abundance of small alluvial fans in the Appalachian Mountains (Kochel, 1990; Jennings and others, 2003), the surficial maps of the Great Smoky Mountains National Park (Southworth and others, 2003) show that fans cover less than 20 percent of the surface, mostly in lower slope positions. Regolith is generally transported slowly down slope by diffusive processes; thus, we suspect that the long residence time of colluvium on the moist and densely vegetated slopes allows rock fragments to weather and break down to sand-size grains during down-slope transport.

The slope angles in the Great Smoky Mountains, defined by the analysis of a 30 m DEM, are in the range of those studied by Mills (2000b) in the North Carolina Blue Ridge. At angles ranging between 19° to 27°, typical of the Great Smoky Mountains, Mills (2000b) found that hill slope deposits range from sandy colluvium to talus material consisting of a boulder and sand mix. Once the sandy colluvium reaches the stream, it is rapidly transported out of the mountain range. The water in the Great Smoky Mountain rivers is generally clear, even during high discharge events, suggesting that sediment yields are low. Together, our field observations suggest the dominance of slow slope processes in the Great Smoky Mountains. Thus, we conclude that most of the cosmogenic nuclides we measured in the fluvial sediments accumulated while the material was on the hill slopes rather than in the stream system, an assertion supported by the nuclide data.

Cosmogenic Nuclides in Erosion Studies

Cosmogenic nuclides have been used to estimate rates of erosion at discrete locations on the landscape (for example, Nishiizumi and others, 1986; Small and others, 1999; Bierman and Caffee, 2001, 2002), rates of sediment production from individual drainages (for example, Brown and others, 1995; Granger and others, 1996; Clapp and others, 2000, 2001, 2002; Bierman and others, 2001; Schaller and others, 2001), and rates of soil production (Heimsath and others, 1997, 1999, 2001). Cosmogenic nuclide concentrations in sediments reflect basin-wide average cosmic-ray exposure history (Brown and others, 1995; Granger and others, 1996; Bierman and Steig, 1996). Rates of erosion can be quantified using a model beholden to a variety of assumptions including constant rates of erosion, constant or minimal sediment storage within the sampled basin, homogeneous quartz distribution, and thorough mixing of sediment (Bierman and Steig, 1996; Granger and others, 1996). Our field observations, mass balance calculations based on cosmogenic nuclide measurements (Matmon and others, 2003), and previously published data (Hadley and Goldsmith, 1963; King, 1964) suggest that the Great Smoky Mountains generally meet these assumptions.

^{10}Be and ^{26}Al concentrations in alluvial sediments have been shown to be useful tools for understanding various aspects of landscape development by numerous investigators. Granger and others (1996) calculated basin-wide erosion rates from cosmogenic nuclides measured in desert alluvial sediments that match integrated erosion rates inferred from dated fans of known volume. Brown and others (1995) used ^{10}Be measurements in sediments from a small watershed in Puerto-Rico to distinguish sources of different sized sedimentary particles as well as to calculate erosion rates that match, within a factor of 2, modern sediment yields for the basin they studied. They concluded that particles larger than 1 millimeter were contributed by mass wasting events and those smaller than 1 millimeter were contributed by the continuous weathering of bedrock to soil. Dependence of nuclide concentrations on grain size was not detected by later studies in arid environments (Clapp and others, 2000, 2001, 2002). Schaller and others, 2001, who found a slight grain-size dependence of cosmogenic nuclide concentrations, concluded that average cosmogenically derived erosion rates were similar to long-term rock uplift rates in middle Europe, that hillslope sediment transport is dominated by diffusive processes, and that lithology influences erosion rates.

The measurement of cosmogenic nuclide concentration in alluvial sediments enables the comparison between short-term (10^1-10^2) and long-term (10^3-10^5) rates of sediment generation (Brown and others, 1995; Granger and others, 1996; Nott and Roberts, 1996; Clapp and others, 2000, 2001; Kirchner and others, 2001; Schaller and others, 2001; Bierman and others, 2001). Some studies find that nuclide-determined sediment generation estimates exceed traditionally measured sediment yields in

tectonically active mountain ranges (Kirchner and others, 2001; Bierman and others, 2001) and in densely populated, partially glaciated regions (Schaller and others, 2001). These results imply that large sediment transport events are missed by the short gauge record. Conversely, other studies find that sediment yields exceed cosmogenically estimated sediment generation rates (Brown and others, 1995; Clapp and others, 2000, 2001) implying that stored sediment is being mined. Some studies find that erosion rates measured both ways are similar (Granger and others, 1996; Nott and Roberts, 1996), suggesting that erosion rates integrated over different time frames are similar. In the few places where cosmogenically derived rates of sediment generation have been compared with longer term rates of uplift deduced by thermochronometers, the results are usually similar (Cockburn and others, 2000; Bierman and Caffee, 2001; Kirchner and others, 2001; Matmon and others, 2003; Vance and others, 2003)

Testing parameters that control erosion on a basin scale is also possible. Riebe and others (2000, 2001a, 2001b) sampled alluvial sediments from small catchments at seven sites in the Sierra Nevada and tested the relation between basin-wide average erosion rates and proximity to regions of rapid base level lowering as well as climate. They concluded that the most important factor controlling erosion is the rate at which base level changes. Climatic factors appeared to be of secondary importance.

METHODS

Sample Collection

To understand the pattern of erosion throughout the Great Smoky Mountains, we collected several types of samples (table 1, figs. 4 and 5): bedrock (n=10), colluvium (n=3), and fluvial sediments (n=43). These samples, and additional grain size splits of some sediment and colluvium samples, were analyzed to determine the concentration of ^{10}Be, and in most samples, ^{26}Al.

Exposed bedrock.—The analysis of cosmogenic ^{26}Al and ^{10}Be concentrations in bedrock outcrops provides bedrock-lowering rates at specific locations in the present topography. Since most of the ridge tops in the Great Smoky Mountains are soil-covered, bedrock outcrops are rare. Samples were collected from outcrops on the main Great Smoky Mountain drainage divide and along the Cataloochee River-Raven Fork divide (fig. 4). All samples were taken on or within several meters of local divides except for sample GSC-3, which was collected from an outcrop on a slope about 70 meters below the ridge top in the Raven Fork drainage basin.

Most bedrock samples were collected from metamorphosed sandstone outcrops. Samples GSDV-6 and SDV-11 were collected from quartz pegmatites. The pegmatites did not stand above the adjacent sandstone. Sample GSC-3 was collected from a gneiss outcrop. Sampled bedrock outcrops were 1 to 4 meters higher than the soiled-covered surface around them (fig. 2F). Samples were taken from the upper flat surface of the outcrops and sample thickness was $\leq$ 5 centimeters. There is no field evidence for exfoliation of the outcrops and they seem to erode in a continuous, grain-by-grain process.

Colluvium.—Colluvium samples were collected in order to examine the residence time of relatively coarse material on the slope. Samples GSDV-5 and GSDV-9 are ridge-top samples (fig. 4). They were collected, respectively, from around the outcrops where bedrock samples GSDV-4 and GSDV-8 were collected. Samples GSDV-5 and GSDV-9 were separated into 0.25 to 2 and >2 millimeter fractions to test whether nuclide concentration varied with grain size. Sample GSC-4 was collected along contour ~70 meters below bedrock sample GSC-3. It is a slope sample (fig. 4) consisting of several hundred rock fragments (1 to 2 cm in diameter) that were mixed. Pure quartz fragments were avoided in order not to overwhelm the sample with quartz from a single location.

TABLE 1

Sample locations—Great Smoky Mountains

Sample name	Basin name	Longitude (UTM)[1]	Latitude (UTM)[1]	Sampling elevation (masl)	Basin area (km^2)[2]	Sample type
GSRF-1	Raven Fork	0295743	3942840	1090	37	Sediment
GSRF-2	Ledge Creek	0301349	3944775	1100	1.4	Sediment
GSRF-3	Ledge Creek	0301349	3944775	1100	1.0	Sediment
GSRF-5	Ledge Creek	0300781	3944187	1030	1.0	Sediment
GSRF-6	Straight Fork	0299677	3944114	960	27	Sediment
GSRF-7	Ledge Creek	0299969	3943633	980	7.7	Sediment
GSRF-8	Straight Fork	0299518	3943186	940	3.6	Sediment
GSRF-9	Straight Fork	0298548	3942529	910	2.9	Sediment
GSRF-10	Straight Fork	0297176	3939957	920	52	Sediment
GSRF-11	Raven Fork	0294868	3939549	800	56	Sediment
GSRF-12	Raven Fork	0291862	3932549	630	192	Sediment
GSRF-13	Bunches Creek	0296372	3937337	760	42	Sediment
GSCO-1	Oconaluftee	0291319	3931360	640	330	Sediment
GSCO-1A	Oconaluftee	0291319	3931360	640	330	Sediment
GSCO-2	Oconaluftee	0290852	3932532	640	135	Sediment
GSCO-3	Oconaluftee	0290710	3932985	650	9.4	Sediment
GSCO-4	Oconaluftee	0290398	3937215	700	51	Sediment
GSCO-5	Oconaluftee	0288276	3938250	740	12	Sediment
GSCO-6	Oconaluftee	0286247	3940454	870	3.3	Sediment
GSCO-7	Oconaluftee	0281413	3942223	1230	2.3	Sediment
GSLR-1	Little River	0254927	3949542	360	156	Sediment
GSLR-2	Little River	0272163	3942248	990	8	Sediment
GSLR-3	Little River	0272081	3942329	1070	15	Sediment
GSLR-4	Little River	0270849	3944114	920	6	Sediment
GSLR-5	Little River	0269757	3944107	870	30	Sediment
GSLR-6	Little River	0266234	3948211	670	12	Sediment
GSLR-7	Little River	0265313	3949634	640	100	Sediment
GSBC-1	Big Creek	0308730	3958027	500	75	Sediment
GSBC-2	Big Creek	0307342	3956512	730	66	Sediment
GSCS-1	Cosby Creek	0300560	3958663	700	7.1	Sediment
GSCS-2	Cosby Creek	0300529	3958622	700	0.8	Sediment
GSLP-1	Little Pigeon	0281639	3957206	430	117	Sediment
GSMP-1	Middle Prong	0254696	3949286	360	118	Sediment
GSWP-1	West Prong	0270544	3952039	500	64	Sediment
GSDC-1	Deep Creek	0279101	3927035	560	105	Sediment
GSAC-1	Abram's Creek	0234078	3944424	350	158	Sediment
GSPB-1	Parsons Branch	0233897	3932192	430	15	Sediment
GSTM-1	Twenty Mile	0238819	3928425	380	39	Sediment
GSNC-1	Nolan Creek	0270636	3926601	590	47	Sediment
GSCA-1	Cataluchee River	0312519	3949004	810	150	Sediment
GSFC-1	Forney Creek	0267061	3927518	690	72	Sediment
GSHC-1	Hazel Creek	0253395	3928378	550	116	Sediment
GSEC-1	Eagle Creek	0248544	3930507	570	58	Sediment
GSC-3	Straight Fork	0297169	3943423	1250	NA	Rock - Gneiss
GSC-4	Straight Fork	0297169	3943423	1250	NA	Coluvium - below GSC-3
GSDV-1	Oconaluftee, Little Pigeon	0280685	3943354	1620	NA	Rock - Thunderhead Sandstone
GSDV-2	Big Creek, Cosby Creek	0302099	3955965	1570	NA	Rock - Thunderhead Sandstone
GSDV-3	Big Creek, Cosby Creek	0297600	3955750	1750	NA	Rock - Thunderhead Sandstone
GSDV-4	Big Creek, Raven Fork, Little Pigeon	0294992	3951532	1900	NA	Rock - Thunderhead Sandstone
GSDV-5	Big Creek, Raven Fork, Little Pigeon	0294668	3951460	1900	NA	Colluvium - around GSDV-4
GSDV-6	Raven Fork, Little Pigeon	0292299	3948553	1800	NA	Rock - Quartz pegmatite
GSDV-7	Oconaluftee, Little Pigeon	0284339	3945833	1700	NA	Rock - Anakeesta Sandstone
GSDV-8	Little River, Nolan Creek, Forney Creek	0273137	3938070	2010	NA	Rock - Thunderhead Sandstone
GSDV-9	Little River, Nolan Creek, Forney Creek	0273331	3938095	2030	NA	Colluvium - around GSDV-8
GSDV-10	Mt. Sterling Big Creek, Cataloochee Creek	0307713	3952348	1750	NA	Rock - Thunderhead Sandstone
GSDV-11	Ledge Creek, Cataloochee Creek	0302505	3945542	1410	NA	Rock – Quartz pegmatite

[1]Measured with Garmin 12; referenced to NAD 27; [2]area upstream of sampling point; NA—not applicable.

Alluvium.—Alluvial sediment samples were collected for estimation of basin scale erosion rates, to detect downstream trends in cosmogenic nuclide concentration, and to test whether basin scale parameters (such as lithology, aspect, climate, and gradient) control erosion rates. Sediment was sampled from most of the outlet rivers (n=18, fig. 4) in the Great Smoky Mountains. Together, these basins drain 80 percent of the range's area. Sample GSCO-1 was taken below the confluence of the Raven Fork and the Oconaluftee River to test how well sediment from the two rivers was mixed. Sample GSCO-1A is a temporal replicate of GSCO-1; it was collected from the same location 4

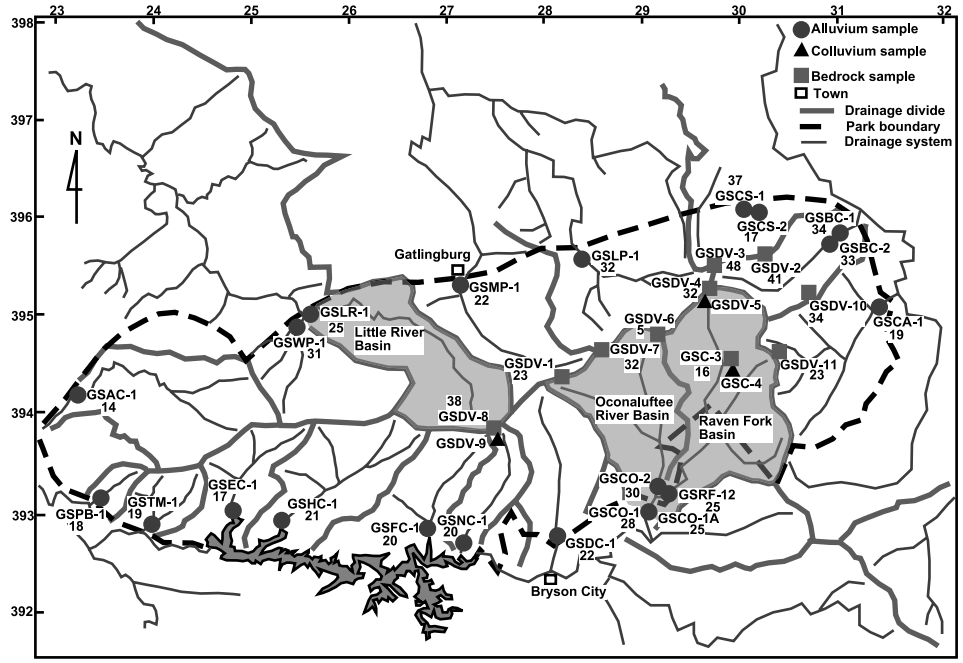

Fig. 4. Sampling locations in the Great Smoky Mountains (UTM grid). Numbers near sample names are model erosion rates (mm Ky^{-1}) calculated from ^{10}Be concentrations. GSBC-2 is a replicate sample of GSBC-1. GSCO-1A is a replicate sample of GSCO-1. Samples GSCO-1, GSCO-1A, GSLR-7 (fig. 5), GSBC-2, GSCS-1, and GSCS-2 were not considered outlet rivers in the calculation of mean erosion rates.

months after sample GSCO-1. Sample GSBC-2 was taken as a replicate of sample GSBC-1. Both were collected on the same day, about 1 kilometer from each other. Two samples, GSAC-1 from Abrams Creek and GSCS-2 from the Cosby Fan, were collected from locations that have significant sediment storage to test for any effect of such storage on cosmogenic nuclide concentrations in present-day stream sediments. Samples GSCO-1, GSCO-1A, GSBC-2, and GSAC-1 were not included in the calculation of the outlet rivers for reasons described above. Sample GSLR-7 was also not included. It was taken from the main stem of the Little River several kilometers upstream of sample GSLR-1 to enable mass balance calculations of sediment yield in the Little River drainage basin.

All alluvial sediment was collected from within river channels or from sandbars (fig. 2C, D). Sand was collected and mixed from several locations across the channel. Sediment was sieved and the 0.25 to 0.85 millimeter fraction was analyzed for cosmogenic nuclide concentration. Six samples were separated into size fractions (0.25 to 0.85, 0.85 to 2, 2 to 10, >10 mm) to test whether different size grains have different cosmogenic nuclide concentrations and to relate such differences to erosional processes (Brown and others, 1995). Within three basins, we sampled major tributaries in detail (Oconaluftee River, n=5; Raven Fork, n=11; Little River, n=6, fig. 5) to test the assumptions of thorough sediment mixing, minor alluvial storage, and to locate sediment sources.

Isotopic Analysis

Cosmogenic samples were processed following the method described in Bierman and Caffee (2001). ^{26}Al and ^{10}Be were measured at the Center for Accelerator Mass

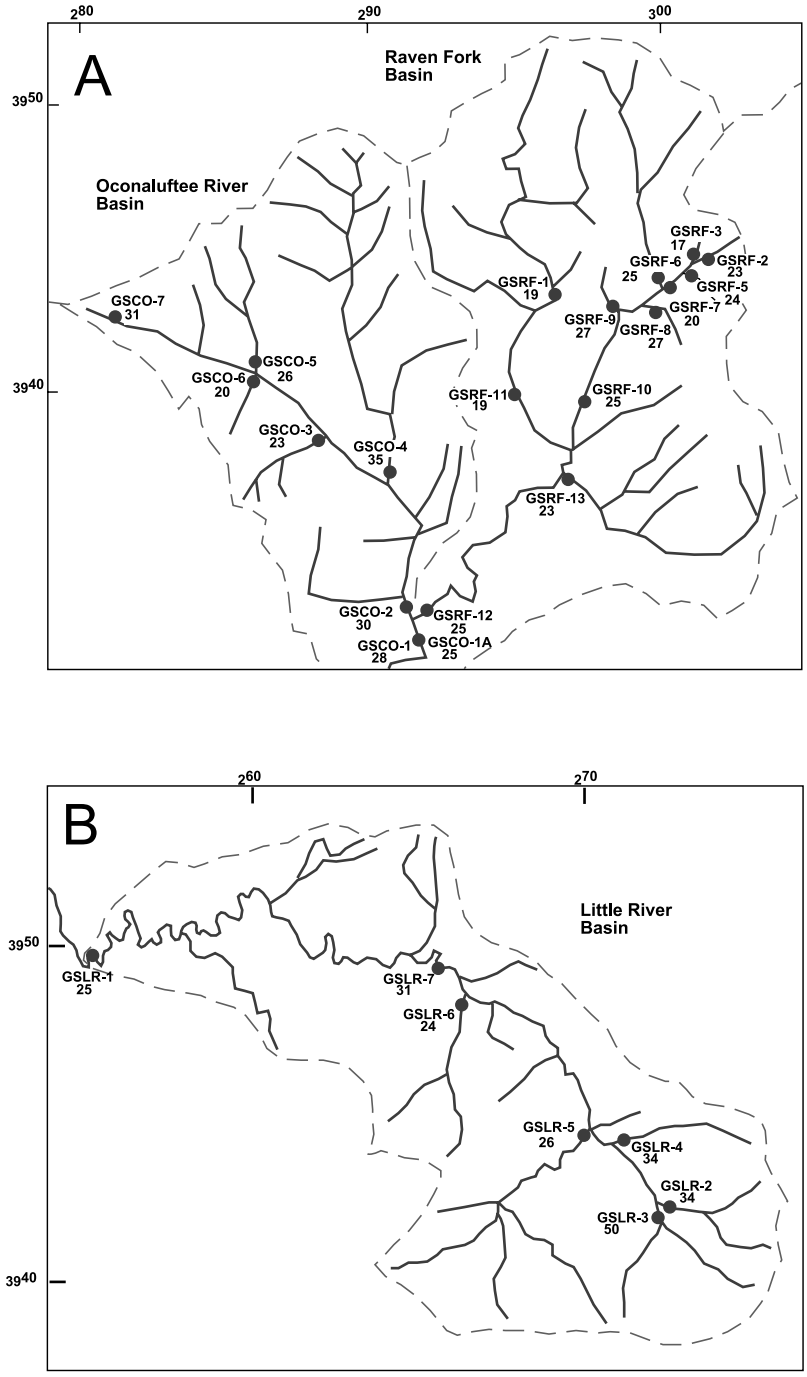

Fig. 5. Location (UTM grid) of detailed tributary sampling in the Oconaluftee River (A), Raven Fork (A), and Little River (B). Numbers under sample name are erosion rates in mm Ky^{-1} calculated from ^{10}Be concentrations. Samples GSCO-1, GSCO-1A, and GSLR-7 were not considered outlet rivers in the calculation of mean erosion rates.

Spectrometry (AMS) at Lawrence Livermore National Laboratory. Erosion rates were calculated considering nucleongenic isotopes only and a sea-level high–latitude production rate of 5.17 ^{10}Be atoms g^{-1} quartz yr^{-1} (Bierman and others, 1996; Stone, 2000; Gosse and Stone, 2001). Latitude/altitude scaling of the nucleonic production rate was done using Lal (1991). We realize that some other studies (for example, Schaller and others, 2001) have included the muogenic production in their erosion rate calculations for sediment samples. However, since we do not yet know where most dosing of our sampled sediments occurred, as buried bedrock or near-surface soil, we can not assume steady denudation as a model. Indeed, if most dosing occurs in shallow soils, then muons account for no more than 4 percent of the cosmogenic production (Braucher and others, 2003). If we calculated bedrock erosion rates using the approach of Braucher and others (2003), they would be ~10 percent higher. However, in order to enable the comparison of erosion rates derived from bedrock samples to those derived from sediment samples and in order to allow the comparison of results from this study to results from numerous other papers, we do not include the muogenic contribution in our erosion rate calculations. Equation 1 was used to calculate bedrock erosion rates (Lal, 1988):

$$N = \left(P_{(n)} \Big/ \left(\frac{\varepsilon\rho}{\Lambda_{(n)}} + \lambda \right) \right) \tag{1}$$

Where N = measured concentration (atoms g^{-1} quartz), P = site specific production rate (atoms g^{-1} quartz yr^{-1}) by neutrons (n), ε = erosion rate (cm yr^{-1}), ρ = density of sampled material (g cm^{-3}), λ' the decay constant (yr^{-1}), and Λ = attenuation depth (g cm^{-2}) of neutrons (n).

Basin scale erosion rates were calculated using the method described in Bierman and Steig (1996) and:

$$m/\rho = \varepsilon = \Lambda(P - N)/\rho N$$

Where P = basin effective production rate (atoms g^{-1} quartz yr^{-1}) and m = sediment generation rate (g yr^{-1}cm^{-2}). We assume that erosion rates are fast enough to consider ^{26}Al and ^{10}Be as stable isotopes (Brown and others, 1995; Bierman and Steig, 1996). To interpret the nuclide data for alluvial sediments, basin-integrated nuclide production rates were estimated. The hypsometery of each basin was divided into 100-meter elevation bins, the effective cosmogenic nuclide production rate was calculated at the mid-elevation of each bin, and an area-weighted average production rate was calculated (Brown and others, 1995; Bierman and Steig, 1996; Granger and others, 1996). For large basins (>50 km^2), we determined basin hypsometry and calculated effective or integrated nuclide production rates using Digital Elevation Models (DEM). For small basins, we digitized 1:100000 topographic maps. The analytic precision of the measured samples, considering AMS and stable nuclide concentrations, is 3 to 5 percent (1σ). We propagate a 10 percent (1σ) uncertainty in production rates when making erosion rate calculations. We did not specifically correct for variations in Earth's magnetic field, topographic shielding, errors associated with the enrichment of quartz in the alluvial system, and muon production at depth.

Morphometry

River profiles were digitized from 1:24000 topographic maps. Geological and structural data (Hamilton, 1961; Hadley and Goldsmith, 1963; King, 1964; King and others, 1968) were added to the profiles to test the relation between longitudinal profiles, lithology, and structure. GIS procedures were used to derive physical parameters for each sampled basin including: mean elevation, maximum elevation, maximum relief (the elevation difference between the highest point in the basin and the

sampling point), relief ratio (ratio between the relief and distance between the highest and lowest points of the trunk channel), drainage basin area, mean slope gradient, and drainage density (km of channel per km^2 of basin area). These various parameters were correlated with model rates of erosion and ^{10}Be concentrations to assess their influence on the spatial pattern of cosmic-ray dosing, and by inference, erosion in the Great Smoky Mountains.

For the GIS analysis, a digital elevation model (DEM; 30 X 30 meter grid) of the Great Smoky Mountain region (supplied by the USGS) was used as the base layer from which streams, watersheds, and slope grids were developed. Using ArcView in combination with Prepro 0.3, the DEM was used to create a stream network as well as a watershed coverage. The Prepro program contains steps for modifying the DEM by filling sinks, computing flow direction, computing flow accumulation, and delineating stream networks. Delineating the stream networks requires specifying a threshold of DEM grid cells that defines the beginning of a stream. A threshold for stream definition of 100 cells (90000 m^2) was used to create a stream network from the DEM.

Using the delineated stream network and the location of samples, the sampled watersheds were identified in the DEM. In each basin, elevation was divided into 100-meter bins. For example, the 100 to 200 meter bin consisted of all the cells that have an elevation value between 100 and 200 meters above sea level. The mid-elevation of each bin was used to calculate the production rate of the bin. The number of cells in each bin was counted, the area of each bin was calculated relative to the total area of the basin, and the effective production rate of the basin was calculated by weighting the bin area relative to the basin area. Slope gradient distribution was calculated within each sampled basin. Local slope gradient was derived from the DEM using ArcView and the Spatial Analyst extension. The slope is derived by determining the maximum rate of elevation change between a grid cell and its neighbors within the DEM. Slope length was determined by the number of accumulated cells along a flow line before entering the streams. Drainage density was determined as the ratio between the total length of streams within each basin and the basin's area.

Data

Cosmogenic Results

Bedrock samples.—Bedrock samples from the Great Smoky Mountain (n=10) were collected from sandstone, gneiss, and quartz pegmatites (tables 1 and 2). The seven samples that were taken from sandstone of various formations yield an average normalized ^{10}Be concentration of $0.093 \pm 0.023 \times 10^6$ atoms g^{-1} quartz. The normalized ^{10}Be concentrations in the samples collected from the other lithologies were higher (table 2).

Colluvium samples.—^{10}Be concentrations in colluvium samples, and their relation to adjacent bedrock outcrops, offer no consistent spatial or temporal framework for the formation and movement of colluvium. The different grain fractions from samples GSDV-5 and GSDV-9 yielded similar ^{10}Be and ^{26}Al concentrations (table 2), implying that all grain size fractions of colluvium have similar dosing histories. Sample GSC-4, which was sampled ~70 meters below outcrop sample GSC-3 ($0.470 \pm 0.015 \times 10^6$ atoms g^{-1} quartz), yielded lower ^{10}Be concentration ($0.173 \pm 0.012 \times 10^6$ atoms g^{-1} quartz) than the outcrop (fig. 6). The average ^{10}Be concentration of both grain sizes (0.25 to 2 and >2 mm) of sample GSDV-9 was $0.319 \pm 0.011 \times 10^6$ atoms g^{-1} quartz, similar to that of the outcrop sample GSDV-8 ($0.346 \pm 0.013 \times 10^6$ atoms g^{-1} quartz). Sample GSDV-5, which was collected around the outcrop sample GSDV-4 (^{10}Be concentration of $0.371 \pm 0.018 \times 10^6$ atoms g^{-1} quartz), yielded a higher grain-sized averaged ^{10}Be concentration of $0.740 \pm 0.020 \times 10^6$ atoms g^{-1} quartz.

TABLE 2

Cosmogenic nuclide results for Great Smoky Mountain bedrock and colluvial samples

Sample name and type	Measured ^{10}Be (10^6 atoms g^{-1})[1]	Measured ^{26}Al (10^6 atoms g^{-1})[1]	^{26}Al/^{10}Be	^{10}Be (SL, >60°) (10^6 atoms g^{-1})[2]	^{26}Al (SL, >60°) (10^6 atoms g^{-1})[2]	Normalization factor[3]
GSC-3 (B)	0.470±0.015	2.80±0.13	5.95±0.32	0.197±0.005	1.17±0.06	2.39
GSC-4	0.173±0.012	1.07±0.07	6.17±0.48	0.073±0.003	0.447±0.029	2.39
GSDV-1 (B)	0.431±0.008	2.54±0.14	5.89±0.39	0.138±0.005	0.812±0.044	3.12
GSDV-2 (B)	0.221±0.008	N.D.	N.D.	0.077±0.003	N.D.	3.00
GSDV-3 (B)	0.216±0.007	N.D.	N.D.	0.065±0.002	N.D.	3.41
GSDV-4 (B)	0.371±0.018	2.08±0.12	5.61±0.42	0.098±0.005	0.548±0.031	3.79
[4] (0.25-2) GSDV-5	0.726±0.020	4.91±0.24	6.75±0.38	0.197±0.005	1.33±0.06	3.68
[4] (>2) GSDV-5	0.755±0.023	4.69±0.23	6.21±0.36	0.205±0.006	1.27±0.06	3.68
GSDV-6 (B)	2.17±0.07	13.4±0.7	6.17±0.36	0.613±0.019	3.78±0.19	3.53
GSDV-7(B)	0.297±0.008	N.D.	N.D.	0.097±0.003	N.D.	3.30
GSDV-8 (B)	0.346±0.013	2.32±0.11	6.71±0.42	0.083±0.003	0.559±0.027	4.08
[4] (0.25-2) GSDV-9	0.333±0.011	2.15±0.12	6.44±0.40	0.079±0.003	0.508±0.027	4.23
[4] (>2) GSDV-9	0.305±0.010	2.14±0.12	7.02±0.45	0.072±0.002	0.507±0.028	4.23
GSDV-10 (B)	0.302±0.010	N.D.	N.D.	0.092±0.003	N.D.	3.41
GSDV-11 (B)	0.410±0.013	2.39±0.11	5.84±0.33	0.158±0.005	0.923±0.043	2.68

[1]Errors are propagated 1σ uncertainties in analytical measurements (AMS, ICP). [2]Normalized by scaling to sea level, high latitude production rate using Lal (1991) for elevation/latitude correction for nucleonic production. [3]Normalization factor is the ratio between the site production rate and sea level, >60° latitude production rate. [4]Grain size in mm. Sample GSC-4 was not divided into grain size fractions. (B)—bedrock samples. Unmarked samples are colluvium samples. N.D.—no data.

Sediment samples.—Sediment samples from the Great Smoky Mountain drainage systems (n=43) were collected from headwater streams and from main outlet rivers (table 3). Normalized ^{10}Be concentrations in headwater tributary basins of the Raven Fork, Little River, and Oconaluftee River (for which there are no upstream samples; n=18) range between 0.064 ± 0.002x10^6 and 0.184 ± 0.005x10^6 atoms g^{-1} quartz (table 3) with an average of 0.120 ± 0.028 atoms g^{-1} quartz. Normalized ^{10}Be concentrations of sediments collected from 16 of the 18 sampled outlet rivers that transport most of the sediment from the Great Smoky Mountains (excluding sample GSAC-1 from Abrams Creek which drains large alluvial deposits in Cades Cove and sample GSCO-1) range between 0.085 ± 0.003x10^6 and 0.179 ± 0.007x10^6 atoms g^{-1} quartz with an average of 0.156 ± 0.036 atoms g^{-1} quartz. The largest river (basin area, 330 km^2) draining the Great Smoky Mountains has a normalized ^{10}Be concentration of 0.119 ± 0.004x10^6 atoms g^{-1} quartz (the average of 0.25 to 0.85 mm grain fraction of samples GSCO-1 and GSCO-1A; table 3) similar to that of the headwater tributaries and the outlet rivers.

Samples from Cades Cove and the Cosby Fan, two areas where alluvial sediment is stored, yielded the highest ^{10}Be concentrations among all collected sediment samples. The Cosby Fan is one of the largest boulder deposits in the Great Smoky Mountains (figs. 2 and 3). GSCS-1 is from the main channel that originates at the water divide and dissects the fan. GSCS-2 was taken from a small stream that drains only the fan. Sample GSCS-1 yielded a normalized ^{10}Be concentration of 0.085 ± 0.002 x10^6 atoms g^{-1} quartz. Sample GSCS-2 yielded a normalized ^{10}Be concentration of 0.179 ± 0.005 x10^6 atoms g^{-1} quartz. This two-fold difference probably arises from the residence time and dosing history of material deposited in the boulder fan. This more heavily dosed material is now being eroded and transported by the stream from which sample GSCS-2 was collected.

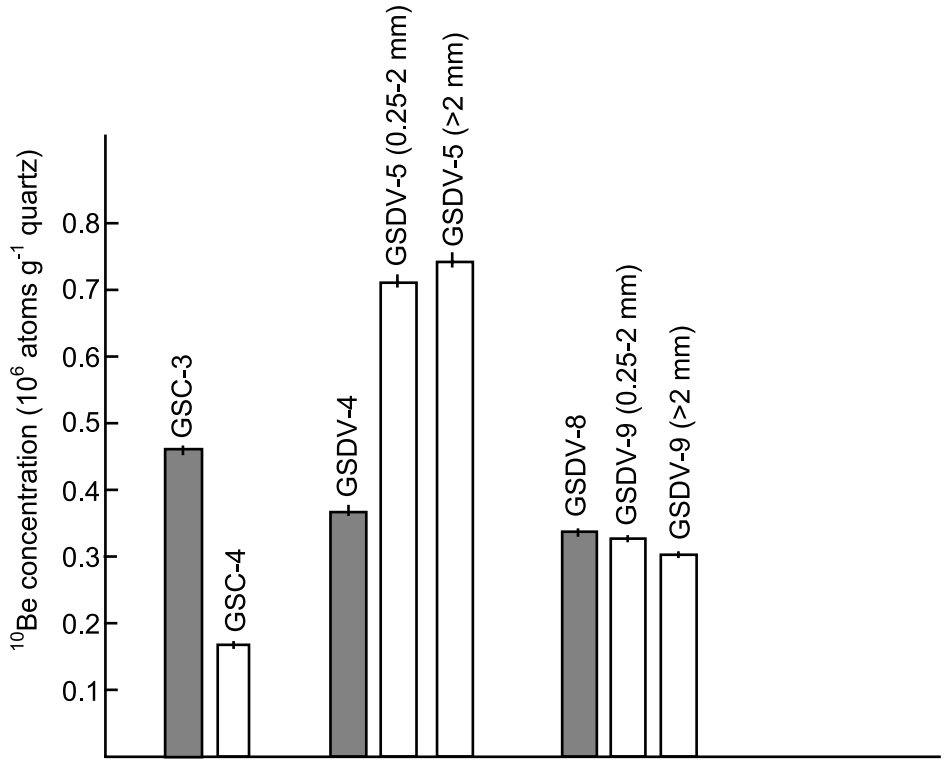

Fig. 6. ^{10}Be concentrations of colluvium samples and their relation to ^{10}Be concentrations of the source outcrop. Shaded bars – bedrock ^{10}Be concentration. Open bars – colluvium ^{10}Be concentration. Colluvium ^{10}Be concentrations can be higher, equal, or lower than ^{10}Be concentrations of the source outcrop and show no grain size difference.

Abrams Creek passes through Cades Cove, one of the few locations within the Great Smoky Mountains where a significant volume of alluvial sediment is stored (fig. 3). A sample from the creek (Sample GSAC-1) yielded a normalized ^{10}Be concentration of 0.218 ± 0.006x10^6 atoms g^{-1} quartz, the highest ^{10}Be concentration of all sediment samples in the Great Smoky Mountains.

^{26}Al to ^{10}Be ratios.—Since ^{26}Al and ^{10}Be are produced with a ratio of ~6 (Nishiizumi and others, 1989) but decay at different rates, their measured ratio can be used to detect burial periods during and after exposure (Lal and Arnold, 1985; Klein and others, 1986; Nishiizumi and others, 1991; Bierman and others, 1999; Bierman and Caffee, 2001; Granger and Muzikar, 2001). The average ^{26}Al/^{10}Be ratio in all samples analyzed for both nuclides (n =54) is 5.8 ± 0.5 (1 standard deviation), indicating no significant burial. However, there are differences between groups. Alluvial samples (n=43) have an average ^{26}Al/^{10}Be ratio of 5.7 ± 0.4 (whether the larger than 0.25 - 0.85 mm grain fractions are included or not; n=32), which is significantly different ($p < 0.01$) from colluvial samples (n=5 including grain size splits) that have an average ^{26}Al/^{10}Be ratio of 6.5 ± 0.4 and from bedrock samples (n=6) that have an average ^{26}Al/^{10}Be ratio of 6.0 ± 0.4 ($p=0.04$). Bedrock and colluvium ^{26}Al/^{10}Be are indistinguishable ($p=0.1$).

Grain size test.—In five of six samples tested, cosmogenic nuclide concentration varies systematically with grain size; smaller grain sizes yield higher ^{10}Be concentrations

TABLE 3

Cosmogenic nuclide results for Great Smoky Mountain sediment samples

Sample name	Measured ^{10}Be (10^6 atoms g^{-1})[1]	Measured ^{26}Al (10^6 atoms g^{-1})[1]	^{26}Al/^{10}Be	^{10}Be (SL, >60°) (10^6 atoms g^{-1})[2]	^{26}Al (SL, >60°) (10^6 atoms g^{-1})[2]	Normal-iztion factor[3]
[4]GSRF-1 (T)	0.434±0.011	2.46±0.12	5.66±0.31	0.161±0.004	0.914±0.045	2.69
[4]GSRF-2 (T)	0.335±0.009	1.87±0.09	5.58±0.30	0.137±0.004	0.766±0.037	2.44
[4]GSRF-3 (T)	0.461±0.012	2.52±0.13	5.47±0.32	0.184±0.005	1.00±0.05	2.51
[4]GSRF-5 (T)	0.322±0.009	2.04±0.10	6.33±0.36	0.132±0.004	0.833±0.041	2.45
[4]GSRF-6 (T)	0.341±0.009	1.81±0.09	5.31±0.29	0.125±0.004	0.662±0.031	2.74
GSRF-7 (T)	0.376±0.011	2.15±0.12	5.72±0.37	0.153±0.004	0.875±0.051	2.46
[4]GSRF-8 (T)	0.297±0.009	1.33±0.10	4.49±0.37	0.115±0.003	0.516±0.040	2.58
[4]GSRF-9 (T)	0.274±0.008	1.69±0.09	6.18±0.37	0.114±0.003	0.706±0.037	2.40
GSRF-10 (T)	0.325±0.009	1.90±0.11	5.84±0.36	0.127±0.004	0.741±0.041	2.56
GSRF-11 (T)	0.452±0.011	2.68±0.13	5.92±0.32	0.162±0.004	0.956±0.047	2.80
GSRF-12 (O)	0.310±0.009	1.53±0.08	4.94±0.30	0.126±0.004	0.622±0.033	2.47
[4]GSRF-13 (T)	0.300±0.010	N.D.	N.D.	0.134±0.004	N.D.	2.24
[5]GSCO-1 (O)	0.264±0.010	1.48±0.08	5.58±0.39	0.112±0.004	0.624±0.036	2.37
[5,6]GSCO-1A (O)	0.295±0.009	1.54±0.09	5.21±0.35	0.124±0.004	0.646±0.039	2.37
GSCO-2 (O)	0.234±0.007	1.32±0.07	5.64±0.34	0.104±0.003	0.586±0.030	2.25
[4]GSCO-3 (T)	0.312±0.008	1.79±0.09	5.72±0.31	0.134±0.003	0.765±0.037	2.34
[4]GSCO-4 (T)	0.200±0.006	1.06±0.09	5.30±0.49	0.089±0.003	0.473±0.042	2.25
[4]GSCO-5 (T)	0.317±0.008	1.85±0.09	5.83±0.32	0.119±0.003	0.694±0.033	2.67
[4]GSCO-6 (T)	0.361±0.012	2.11±0.11	5.85±0.37	0.154±0.005	0.902±0.048	2.34
[4]GSCO-7 (T)	0.278±0.007	1.72±0.09	6.20±0.38	0.102±0.003	0.636±0.035	2.71
GSLR-1 (O)	0.264±0.007	1.61±0.09	6.11±0.38	0.126±0.003	0.771±0.043	2.10
[4]GSLR-2 (T)	0.256±0.008	1.40±0.09	5.48±0.38	0.093±0.003	0.509±0.032	2.76
[4]GSLR-3 (T)	0.178±0.006	N.D.	N.D.	0.063±0.002	N.D.	2.81
[4]GSLR-4 (T)	0.224±0.007	N.D.	N.D.	0.092±0.003	N.D.	2.43
[4]GSLR-5 (T)	0.301±0.009	N.D.	N.D.	0.121±0.004	N.D.	2.48
[4]GSLR-6 (T)	0.282±0.010	N.D.	N.D.	0.131±0.005	N.D.	2.16
[5]GSLR-7 (O)	0.240±0.008	N.D.	N.D.	0.102±0.003	N.D.	2.35
GSBC-1 (O)	0.234±0.006	1.45±0.09	6.22±0.42	0.093±0.003	0.577±0.036	2.52
[5,6]GSBC-2 (O)	0.247±0.008	1.29±0.08	5.23±0.35	0.095±0.003	0.496±0.029	2.60
[5]GSCS-1 (O)	0.191±0.005	1.13±0.06	5.91±0.35	0.085±0.002	0.503±0.026	2.25
GSCS-2 (T)	0.333±0.009	1.87±0.09	5.62±0.31	0.179±0.005	1.00±0.05	1.87
GSDC-1 (O)	0.316±0.008	1.76±0.09	5.57±0.32	0.145±0.004	0.806±0.041	2.19
GSLP-1 (O)	0.225±0.007	1.28±0.07	5.70±0.36	0.099±0.003	0.561±0.032	2.28
GSMP-1 (O)	0.267±0.007	1.37±0.07	5.12±0.28	0.142±0.004	0.727±0.035	1.88
GSWP-1 (O)	0.242±0.006	1.25±0.07	5.17±0.31	0.101±0.003	0.522±0.028	2.40
[5]GSAC-1 (O)	0.362±0.011	2.16±0.11	5.96±0.34	0.218±0.006	1.30±0.06	1.66
GSPB-1 (O)	0.295±0.012	N.D.	N.D.	0.174±0.007	N.D.	1.71
GSTM-1 (O)	0.309±0.009	N.D.	N.D.	0.161±0.005	N.D.	1.95
GSNC-1 (O)	0.363±0.012	2.11±0.10	5.81±0.33	0.159±0.005	0.927±0.043	2.28
GSCA-1 (O)	0.379±0.011	2.32±0.11	6.14±0.34	0.161±0.005	0.990±0.048	2.35
GSFC-1 (O)	0.359±0.011	N.D.	N.D.	0.158±0.005	N.D.	2.28
GSHC-1 (O)	0.318±0.010	N.D.	N.D.	0.148±0.005	N.D.	2.15
GSEC-1 (O)	0.341±0.011	N.D.	N.D.	0.179±0.006	N.D.	1.91

[1]Errors are 1σ uncertainties in analytical measurements (AMS, ICP). [2]Using basin-wide effective production rate (convolving hypsometric curves and Lal (1991) for elevation/latitude correction without muon production). [3]Normalization factor is the ratio between the basin-wide effective production rate and sea level, >60° latitude production rate. [4]Headwater samples for which there are no upstream samples. [5]Outlet river not included in the calculation of mean outlet erosion rate. [6]Replicate sample. (O)—Outlet rivers of the Great Smoky Mountains. (T)—Tributary of Oconaluftee River (GSCO), Raven Fork (GSRF), Little River (GSLR), and Cosby Creek (GSCS). All sediment samples were analyzed using the 0.25–0.85 mm grain size. N.D.—no data.

than larger grain sizes (fig. 7; table 4). The smaller grain size fractions (0.25 - 0.85 and 0.85 - 2 mm) from all the grain size test samples yielded an average measured ^{10}Be concentration of $0.252 \pm 0.035 \times 10^6$ atoms g^{-1} quartz and an average normalized ^{10}Be concentration of $0.100 \pm 0.019 \times 10^6$ atoms g^{-1} quartz. This normalized concentration is similar to that of the entire suite of alluvial sediments, suggesting that these grain sizes represent well the cosmic ray dosing history of the sediment transported out of the Great Smoky Mountains. The larger grain sizes (2 - 10 mm, >10 mm and >2 mm in samples GSCO-1 and GSCO-7) yielded a large range of measured ^{10}Be concentrations ($0.132 \pm 0.004 \times 10^6$ to $0.305 \pm 0.008 \times 10^6$ atoms g^{-1} quartz) with an average of $0.182 \pm 0.057 \times 10^6$ atoms g^{-1} quartz, lower than that of the smaller grain sizes (table 4, fig. 7). Sample GSCO-7, which was collected from the headwaters of the Oconaluftee River, yielded similar measured ^{10}Be concentrations in all grain size fractions.

Samples GSCO-1 and GSCO-1A, which were collected from the same site 4 months apart, exhibit a difference of ~10 percent in the ^{10}Be concentrations of the small grain sizes (0.25 - 0.85 mm, 0.85 - 2 mm). This difference probably represents the natural cosmogenic nuclide variance within sediments over time. ^{10}Be concentration from the >2 millimeter fraction of sample GSCO-1 is significantly lower ($0.165 \pm 0.004 \times 10^6$ atoms g^{-1} quartz) than the 2 to 10 millimeter fraction of sample GSCO-1A ($0.262 \pm 0.009 \times 10^6$ atoms g^{-1} quartz). However, the largest (>10 mm) fraction of sample GSCO-1A yielded a ^{10}Be concentration of $0.189 \pm 0.006 \times 10^6$ atoms g^{-1} quartz, similar to that of the >2 millimeter fraction of sample GSCO-1. This similarity suggests that most of the grains in sample GSCO-1 (>2 mm) probably were larger than 10 millimeters, and that they dominated the measured ^{10}Be concentration of the sample.

Morphometric Results

Longitudinal profiles.—The longitudinal profiles of the sampled outlet rivers indicate that in most cases, river channels in the Great Smoky Mountains are graded and approach a steady state profile (Whipple, 2001). Most rivers are concave upwards with a steep reach at the headwaters. Several kilometers down stream of the divide, stream gradient decreases. However, there are exceptions. Major knick-points and convex reaches appear in several of the profiles (fig. 8). Most prominent is the knick-point in Raven Fork (fig. 8A), associated with the outcropping of the Grenville Basement. Similar high-gradient reaches appear also in the profiles of Bunches Creek (fig. 8C), Eagle Creek, the Little Pigeon River, the Middle Prong of the Little River (fig. 8B), and the West Prong of the Little Pigeon River.

In the Middle Prong of the Little River, the Little Pigeon River (cross section from Mt. Kephart), and the West Prong of the Little Pigeon River, there is a relation between the convex upward reaches and the underlying Thunderhead Formation sandstone, especially where it crops out adjacent to the less resistant slates of the Anakeesta Formation, suggesting a lithologic control on the stream profile (fig. 8). In Eagle Creek, Little Pigeon River (cross section from Tri-Corner), Bunches Creek, and Twenty Mile Creek there is no apparent lithological explanation for the change in gradient of the stream and for the development of a knick-point. Intraformational variations of the resistance of sandstone to erosion might serve as a possible explanation. Knick-points associated with faults are not seen in the longitudinal profiles, suggesting no recent activity of the faults crossed by the streams.

GIS analysis.—In general, normalized ^{10}Be concentrations are not well correlated with physical parameters of the sampled basins (fig. 9). For example, ^{10}Be concentrations are not correlated with basin relief, drainage area, relief ratio, drainage density, and the distance from the western end of the Great Smoky Mountains National Park (which is a proxy for the precipitation gradient). ^{10}Be concentrations are poorly correlated with basin maximum elevation ($R^2=0.12$; $p=0.02$) and average elevation ($R^2=0.22$; $p<0.01$). A more significant inverse correlation ($R^2=0.42$; $p<0.01$) exists

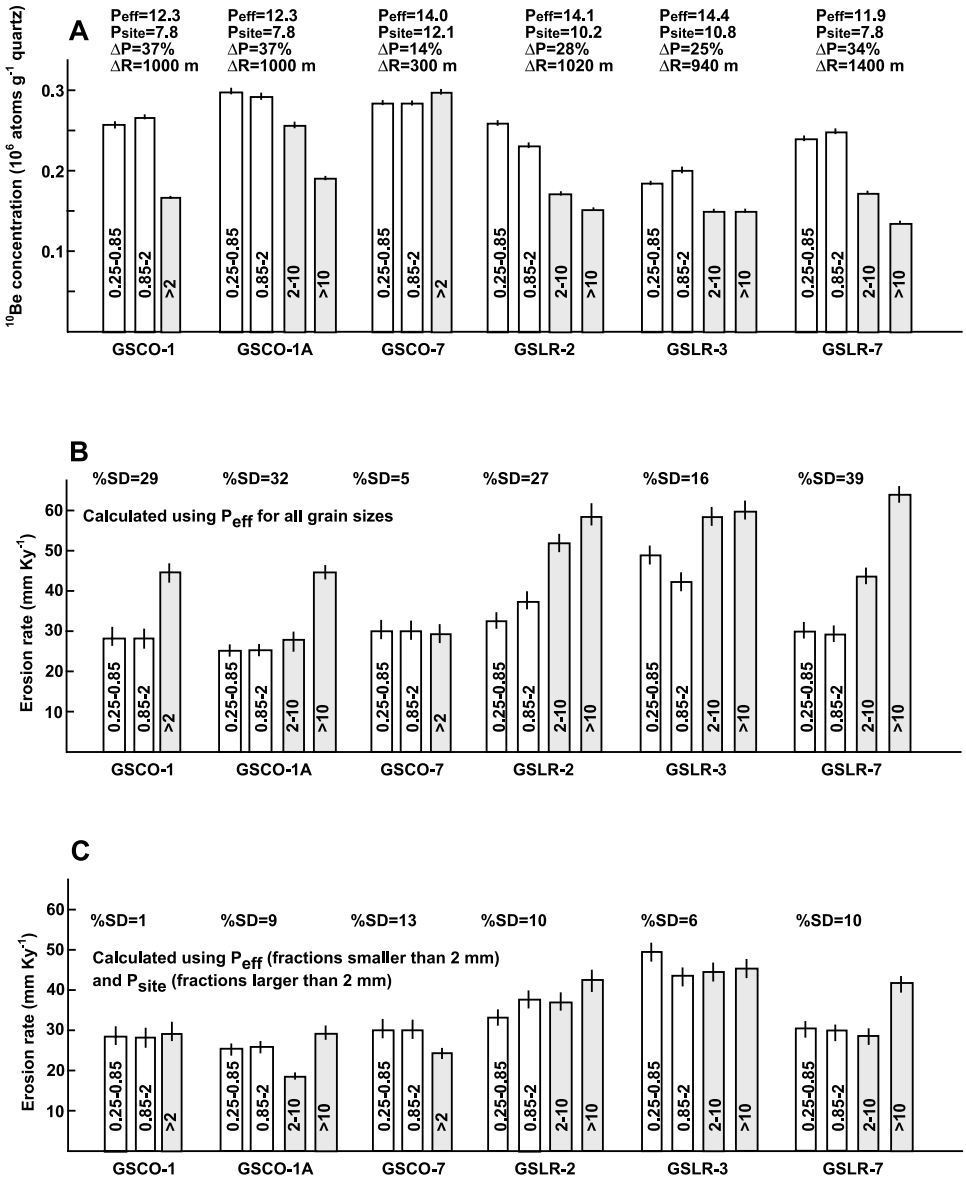

Fig. 7. Results of ^{10}Be analysis of grain size tests in alluvial sediments in the Great Smoky Mountains. Fraction size (mm) written in column. Sample name written below horizontal axis. P_{eff} – Basin wide effective production rate (atoms g^{-1} yr^{-1}) using hypsometric curves. P_{site} – production rate (atoms g^{-1} yr^{-1}) considering sampling site elevation. (A) ^{10}Be concentrations in large fractions (2-10 mm, >10 mm and >2 mm in samples GSCO-1 and GSCO-7) are lower than concentration in smaller fractions, suggesting shorter dosing history or/and lower nuclide production rates. ΔP – the difference between the basin-wide effective production rate (Bierman and Steig, 1996) and the sampling location production rate. Higher ΔP reflects greater relief (ΔR) in the sampled basin. (B) Erosion rates calculated from ^{10}Be concentrations using basin-wide production rates for all size fractions and high-latitude, sea level production rate of 5.17 ^{10}Be atoms g^{-1} quartz yr^{-1}. This calculation results in apparent high erosion rates for large grain sizes. Greater ΔP results in greater differences between the calculated erosion rates of the larger and smaller size fractions. SD = standard deviation. %SD ranges from 5 to 39% of mean (average %SD =25%), indicating the large scatter of erosion rates. (C) Erosion rates calculated from ^{10}Be concentrations using integrated basin-wide production rates for the small grain sizes (0.25-0.85, 0.85-2 mm) which are derived from the entire basin and sampling location production rate for the large grain sizes (2-10 mm, >10 mm, and >2 mm for samples GSCO-1 and GSCO-7). %SD ranges from 1 to 13% of mean (average %SD = 8%) indicating the decrease in scatter of erosion rates compared to 7B.

TABLE 4

Cosmogenic results for grain size test samples, Great Smoky Mountains

Sample name	Size fraction (μm)	Measured ^{10}Be (10^6 atoms g^{-1})[1]	Measured ^{26}Al (10^6 atoms g^{-1})[1]	^{26}Al/^{10}Be
GSCO-1 (O)	250-850	0.264±0.010	1.48±0.08	5.58±0.39
GSCO-1 (O)	850-2000	0.266±0.007	1.46±0.08	5.50±0.33
GSCO-1 (O)	>2000	0.165±0.004	0.961±0.051	5.81±0.35
GSCO-1A (O)	250-850	0.295±0.009	1.54±0.09	5.21±0.35
GSCO-1A (O)	850-2000	0.292±0.010	1.49±0.10	5.10±0.39
GSCO-1A (O)	2000-10000	0.262±0.009	1.36±0.08	5.18±0.36
GSCO-1A (O)	>10000	0.189±0.006	1.21±0.07	6.41±0.42
GSCO-7 (T)	250-850	0.278±0.007	1.72±0.09	6.20±0.38
GSCO-7 (T)	850-2000	0.278±0.007	1.63±0.08	5.87±0.32
GSCO-7 (T)	>2000	0.305±0.008	1.80±0.10	5.90±0.37
GSLR-2 (T)	250-850	0.256±0.008	1.40±0.09	5.48±0.38
GSLR-2 (T)	850-2000	0.230±0.008	1.26±0.07	5.49±0.35
GSLR-2 (T)	2000-10000	0.165±0.006	1.00±0.06	6.07±0.43
GSLR-2 (T)	>10000	0.145±0.005	0.840±0.053	5.79±0.42
GSLR-3 (T)	250-850	0.178±0.006	N.D.	N.D.
GSLR-3 (T)	850-2000	0.202±0.009	N.D.	N.D.
GSLR-3 (T)	2000-10000	0.147±0.005	N.D.	N.D.
GSLR-3 (T)	>10000	0.145±0.006	N.D.	N.D.
GSLR-7 (O)	250-850	0.240±0.008	N.D.	N.D.
GSLR-7 (O)	850-2000	0.245±0.008	N.D.	N.D.
GSLR-7 (O)	2000-10000	0.165±0.005	N.D.	N.D.
GSLR-7 (O)	>10000	0.132±0.004	0.797±0.044	6.02±0.38

[1]Errors are 1σ uncertainties in analytical measurements (AMS, ICP). (O)—Outlet rivers of the Great Smoky Mountains. (T)—Tributary of Oconaluftee River (GSCO) and Little River (GSLR). N.D.—no data.

between ^{10}Be concentrations and basin mean slope gradient. However, a correlation was not found between ^{10}Be concentrations and the mean slope length in each basin. The variability of basin-wide normalized ^{10}Be concentrations (and erosion rates) appears not to be influenced by physical parameters associated with the alluvial systems, but rather with the slope characteristics.

DISCUSSION

Measurements of cosmogenic nuclides provide a new, quantitative means by which to investigate the erosion of an old mountain belt, the Great Smoky Mountains. Nuclide data suggest that erosion is slow and varies little spatially. Together with field observations, our data suggest the importance of slope processes in controlling the production and delivery of sediment to streams draining the range. Data from the Great Smoky Mountains suggest that some aspects of both Hack's and Davis' classic models of Appalachian geomorphic development have some validity.

Erosion Rates

Bedrock and adjacent colluvium.—Nuclide concentrations in bedrock samples (n=10) are consistent with model erosion rates between 48 ± 6 and 5 ± 1 mm Ky^{-1} (^{10}Be) and between 34 ± 5 and 4 ± 1 mm Ky^{-1} (^{26}Al; fig. 4, table 5), with an average of 29 ± 13 (1σ) mm Ky^{-1} for all samples and 34 ± 9 mm Ky^{-1} for sandstone samples. Measured ^{10}Be concentrations of bedrock in the Great Smoky Mountains suggest that on the outcrop scale, relatively resistant lithologies such as quartz pegmatites and gneiss erode more slowly than sandstone.

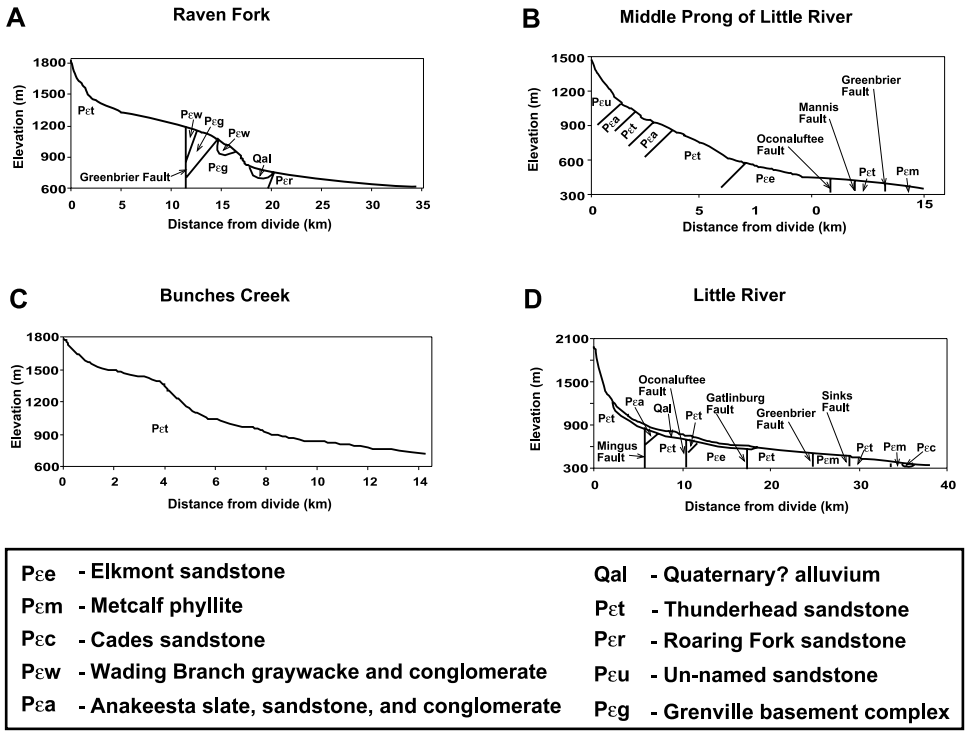

Fig. 8. Selected longitudinal profiles of the sampled rivers in the Great Smoky Mountains. Topography digitized from 1:24000 topographic maps. Knick point location can be correlated with outcrops of resistant rock. (A) Pronounced knick-point in Raven Fork where the Grenville basement rocks crop out. (B) Upward convex reach in the Middle Prong of the Little River where the Thunderhead Formation sandstone crops out and caps Anakeesta Formation slates. (C) In some cases there is no apparent lithologic or structural reason for the existence of the knick-point such as in Bunches Creek. Intraformational variations in resistance to erosion might explain such knick-points. (D) Longitudinal profiles do not suggest recent activity of the faults crossed by the streams such as in the Little River. Geology after Hamilton, 1961; Hadley and Goldsmith, 1963; King, 1964; King and others, 1968.

Siliceous bedrock erosion rates, ranging from <1 to >100 mm Ky^{-1}, have been inferred from cosmogenic nuclide concentrations in several areas around the world including Africa (0.5-15 mm Ky^{-1}), North America (4 - 107 mm Ky^{-1}), Australia (0.3 - 53 mm Ky^{-1}), Antarctica (0.1 - 15 mm Ky^{-1}), and the Middle East (15 - 30 mm Ky^{-1}) (Nishiizumi and others, 1986, 1991; Bierman and Turner, 1995; Bierman and others, 1995; Fleming and others, 1999; Summerfield and others, 1999; Heimsath and others, 1997, 1999, 2000; Small and others, 1999; Cockburn and others, 1999, 2000; Clapp and others, 2000, 2001, 2002; Bierman and Caffee, 2001, 2002). With the exception of the extremely low bedrock erosion rates measured in Antarctica, Australia, and parts of Namibia (<1 mm Ky^{-1}, Nishiizumi and others, 1991; Summerfield and others, 1999; Cockburn and others, 1999, 2000; Bierman and Caffee, 2001, 2002), bedrock erosion rates in the Great Smoky Mountain (5 to 48 mm Ky^{-1}) are in the same range as other measurements. Measured cosmogenic nuclide concentrations in exposed rock are consistent with sediment generation rates between 130 ± 17 and 13 ± 2 tons $km^{-2}\,yr^{-1}$ with an average of 78 ± 34 tons $km^{-2}\,yr^{-1}$ (or 91 ± 23 tons $km^{-2}\,yr^{-1}$ for sandstone when gneiss and quartzite samples, GSC-3 and GSDV-6, are excluded).

Although our sample population is small, the ^{10}Be concentrations in the colluvium samples (n=3) indicates no consistent relationship between cosmogenic nuclide

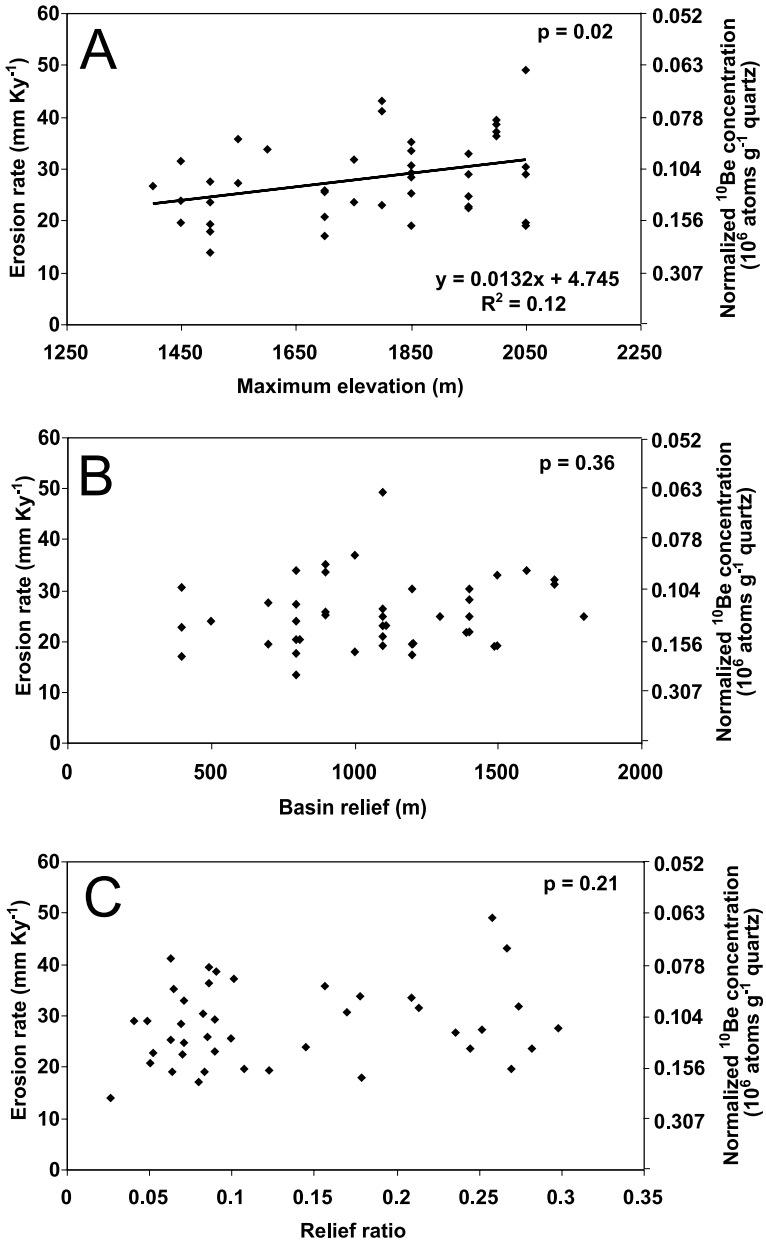

Fig. 9. ^{10}Be normalized concentrations (non-linear scale) and ^{10}Be model erosion rates plotted against various Great Smoky Mountain drainage basin physical parameters. Critical p value is 0.05 (95% confidence). For significant regressions, trend lines and linear regression equations with R^2 value are shown. (A) Weak correlation between erosion rates and basin maximum elevation ($p = 0.02$). (B) No significant correlation between erosion rates and basin relief (elevation difference between highest point in the basin and the sampling location; $p = 0.36$). (C) No correlation between erosion rates and drainage basin relief ratio ($p = 0.21$). Relief ratio is defined as the ratio between the maximum relief and the length of main stem of the river draining the basin. (D) No correlation between erosion rates and drainage basin area ($p = 0.59$). Average erosion rate of the headwater basins (28 ± 7 mm Ky^{-1}, $n=18$), the outlet rivers (24 ± 6 mm Ky^{-1}, $n=15$), and the largest river in the Great Smoky Mountains (26 ± 5 mm Ky^{-1}) are similar indicating the thorough mixing and the rapid movement of sediment in the alluvial channel and suggesting uniform average erosion in all parts of the alluvial system.

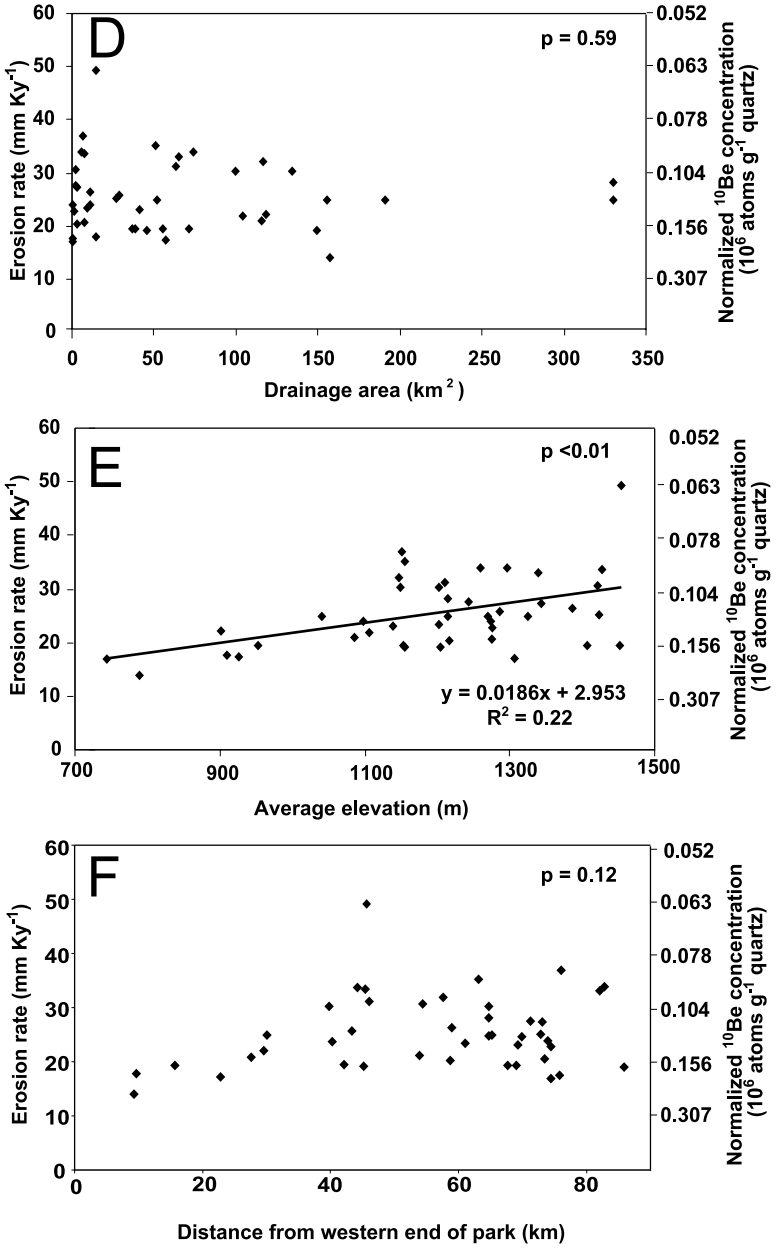

Fig. 9. (continued) (E) Weak correlation between erosion rates and drainage basin average elevation ($p < 0.01$). (F) Erosion rates are not correlated with the distance from the western end of the mountain range ($p = 0.12$). Most of the precipitation in the Great Smoky Mountains is generated by storms approaching from the northwest. (G) Rates of erosion are correlated with the mean slope gradient in each drainage basin ($p < 0.01$) indicating the importance of slope processes in determining erosion rates in the Great Smoky Mountains. (H) No correlation between drainage density (km length of channels per km^2 of basin area) and erosion rates ($p = 0.99$). (I) No correlation between erosion rates and major lithologies that crop out in the basins. Basins that are entirely underlain by the Thunderhead Formation sandstone erode at rates that range from the highest to the lowest measured in this study. (J) No correlation was found between erosion rates and the mean slope length of each basin ($p = 0.79$).

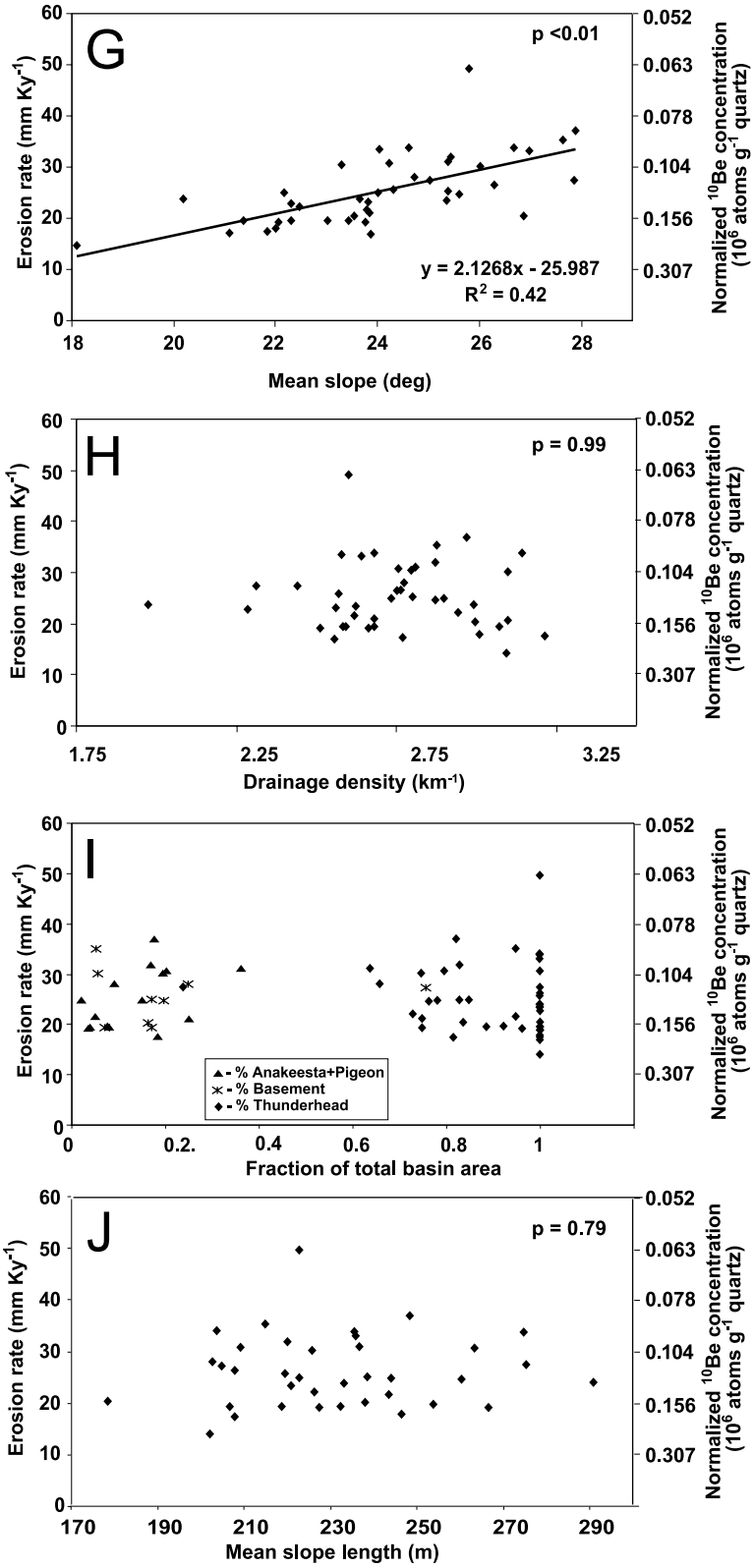

Fig. 9. (continued)

TABLE 5

Interpretation of cosmogenic results for bedrock samples, Great Smoky Mountains

Sample name	^{10}Be model ε (mm Ky^{-1})[1]	^{26}Al model ε (mm Ky^{-1})[1]	^{10}Be Sediment generation rate (tons km^{-2} yr^{-1})[2]	^{26}Al Sediment generation rate (tons km^{-2} yr^{-1})[2]	Lithology
GSC-3	15.8±3.4	15.6±3.5	43±9	42±10	Gneiss
GSDV-1	22.6±2.9	22.5±3.1	61±8	61±8	Sandstone
GSDV-2	40.8±5.3	N.D.	110±14	N.D.	Sandstone
GSDV-3	48.0±6.1	N.D.	130±17	N.D.	Sandstone
GSDV-4	32.0±4.3	33.9±4.7	86±12	92±13	Sandstone
GSDV-6	4.9±0.7	4.4±0.7	13±2	12±2	Quartz pegmatite
GSDV-7	32.4±4.1	N.D.	88±11	N.D.	Sandstone
GSDV-8	37.7±4.9	32.3±4.3	102±13	87±12	Sandstone
GSDV-10	34.2±4.4	N.D.	92±12	N.D.	Sandstone
GSDV-11	23.0±2.9	23.8±3.2	62±8	64±9	Quartz pegmatite

[1]Erosion rates are calculated using Lal (1988) from normalized concentrations and a sea-level, high-latitude production rate of 5.17 ^{10}Be atoms g^{-1} quartz yr^{-1} (Bierman and others, 1996; Stone, 2000; and Gosse and Stone, 2001). Measured concentrations were normalized by scaling to sea level, high latitude production rate using Lal (1991). [2]Sediment generation calculated using density of 2.7 g cm^{-3}. ^{10}Be and ^{26}Al model ε are calculated propagating 10% (1σ) uncertainty in production rates. N.D.—no data.

concentrations in colluvium and adjacent bedrock. Random stirring of sediment through the soil column during down slope movement (Heimsath and others, 2002) probably results in highly variable dosing histories and, thus, variable cosmogenic nuclide concentrations in the different samples relative to nearby exposed bedrock. Exposed bedrock in the Great Smoky Mountains is rare; thus, most bedrock erosion must occur in the subsurface. A much larger and detailed sample population is needed to reveal the relation between bedrock and colluvial dosing histories.

Alluvium.—Using the interpretive models of Brown and others (1995), Granger and others (1996), and Bierman and Steig (1996), ^{10}Be concentrations in alluvial samples are consistent with sediment generation rates between 38 and 133 tons km^{-2} yr^{-1}, the equivalent of continuous surface exposure between 12 ± 1 and 43 ± 5 Ky, and the equivalent of model rock erosion rates between 14 ± 2 and 49 ± 6 mm Ky^{-1} (table 6, fig. 4). ^{26}Al concentrations are consistent with sediment generation rates between 38 and 107 tons km^{-2} yr^{-1}, the equivalent of continuous surface exposure between 15 ± 2 and 43 ± 5 Ky, and the equivalent of model rock erosion rates between 14 ± 2 and 40 ± 6 mm Ky^{-1} (table 6). These data are consistent with the range of short-term rates calculated from river sediment load data for the southeastern United States (Judson and Ritter, 1964).

Model rates of erosion, inferred from cosmogenic nuclide concentrations in Great Smoky Mountain alluvial sediments, indicate spatially homogeneous erosion over a drainage basin-wide scale. Erosion rates in headwater tributary basins of the Raven Fork, Little River, and Oconaluftee River (for which there are no upstream samples; n =18) range from 17 to 49 mm Ky^{-1} (table 6, fig. 5) with an average of 28 ± 8 mMy^{-1}. Basin scale erosion rates, inferred from analysis of sediments collected from the outlet rivers (n =16 excluding samples GSCO-1, GSCO-1A, GSBC-2, GSAC-1, and GSLR-7), which transport most of the sediment from the Great Smoky Mountains, range from 17 to 34 mm Ky^{-1} with an average of 24 ± 6 mm Ky^{-1}. The largest river (basin area, 330 km^2) draining the Great Smoky Mountains has a basin-average erosion rate of 26 ± 5 mm Ky^{-1} (the average of the 0.25 to 0.85 mm grain fraction of samples GSCO-1 and GSCO-1A; table 6) similar to that of the headwater tributaries and the outlet rivers. The consistency of normalized ^{10}Be concentrations and average erosion

TABLE 6

Interpretation of cosmogenic results for sediment samples (250–850 μm fraction) Great Smoky Mountains

Sample name	^{10}Be model ε (mm Ky^{-1})[1]	^{26}Al model ε (mm Ky^{-1})[1]	^{10}Be sediment generation rate (tons km^{-2} yr^{-1})[2]	^{26}Al sediment generation rate (tons km^{-2} yr^{-1})[2]
GSRF-1 (T)	19.3±2.5	20.1±2.7	52±7	54±7
GSRF-2 (T)	22.7±2.9	24.2±3.3	61±8	65±9
GSRF-3 (T)	16.9±2.2	18.1±2.5	46±6	49±7
GSRF-5 (T)	23.7±3.0	21.9±3.0	64 ±8	59±8
GSRF-6 (T)	25.0±3.2	28.0±3.8	68±9	76±10
GSRF-7 (T)	20.4±2.6	20.9±2.9	55±7	56±8
GSRF-8 (T)	27.2±3.5	36.2±5.3	73±10	98±14
GSRF-9 (T)	27.4±3.5	26.0±3.6	74±10	70±10
GSRF-10 (T)	24.6±3.1	24.7±3.4	66±8	67±9
GSRF-11 (T)	19.3±2.4	19.0±2.6	52±7	51±7
GSRF-12 (O)	24.8±3.2	30.0±4.1	67±9	81±11
GSRF-13 (T)	23.3±3.0	N.D.	63±8	N.D.
GSCO-1 (O)	28.0±3.6	29.8±4.1	76±10	80±11
GSCO-1A (O)	24.7±3.2	27.3±3.8	67±9	74±10
GSCO-2 (O)	30.1±3.8	31.8±4.3	81±10	86±12
GSCO-3 (T)	23.3±3.0	24.2±3.3	63±8	65±9
GSCO-4 (T)	35.1±4.5	39.5±6.1	95±12	107±17
GSCO-5 (T)	26.2±3.3	26.7±3.6	71±9	72±10
GSCO-6 (T)	20.2±2.6	20.4±2.8	55±7	55±8
GSCO-7 (T)	30.5±3.9	28.3±3.9	82±11	76±11
GSLR-1 (O)	24.8±3.1	23.3±3.2	67±8	63±9
GSLR-2 (T)	33.8±4.3	36.9±5.2	91±11	100±13
GSLR-3 (T)	49.6±6.3	N.D.	133±17	N.D.
GSLR-4 (T)	33.9±4.3	N.D.	91±12	N.D.
GSLR-5 (T)	25.7±3.3	N.D.	69±9	N.D.
GSLR-6 (T)	23.9±3.1	N.D.	64±8	N.D.
GSLR-7 (O)	30.7±3.9	N.D.	82±10	N.D.
GSBC-1 (O)	33.7±4.3	32.2±4.5	91±12	87±12
GSBC-2 (O)	33.0±4.2	37.6±5.2	89±11	102±14
GSCS-1 (O)	36.9±4.7	37.1±5.0	99±13	100±14
GSCS-2 (T)	17.4±2.2	18.3±2.5	47±6	49±7
GSDC-1 (O)	21.6±2.7	22.2±3.0	58±7	60±8
GSLP-1 (O)	31.8±4.0	32.2±4.2	86±11	87±11
GSMP-1 (O)	22.0±2.8	25.5±3.4	59±8	69±9
GSWP-1 (O)	31.0±3.9	34.6±4.7	84±11	93±13
GSAC-1 (O)	14.2±1.8	14.0±1.9	38±5	38±5
GSPB-1 (O)	17.8±2.4	N.D.	48±6	N.D.
GSTM-1 (O)	19.3±2.5	N.D.	52±7	N.D.
GSNC-1 (O)	19.5±2.5	19.8±2.7	53±7	53±7
GSCA-1 (O)	19.3±2.5	18.5±2.5	52±7	50±7
GSFC-1 (O)	19.8±2.5	N.D.	53±7	N.D.
GSHC-1 (O)	21.1±2.7	N.D.	57±7	N.D.
GSEC-1 (O)	17.4±2.2	N.D.	47±6	N.D.

[1]Erosion rates calculated using Bierman and Steig (1996), from normalized concentrations using basin-wide production rates. [2]Sediment generation rates calculated using density of 2.7 g cm^{-3}. (O)—Outlet rivers of the Great Smoky Mountains; (T)—Tributaries of Oconaluftee River (GSCO), Raven Fork (GSRF), and Little River (GSLR). Erosion rates calculated using sea-level, high-latitude ^{10}Be production rate of 5.17 atoms g^{-1} yr^{-1} supported by data from Bierman et al. (1996), Stone (2000), and Gosse and Stone (2001), and normalized for latitude and elevation using nucleon-only scaling of Lal (1991). ^{10}Be and ^{26}Al model ε are calculated propagating 10% (1σ) uncertainty in production rates. N.D.—no data.

rates with increasing basin area (fig. 9D) suggests thorough downstream sediment mixing and rapid movement of sediment through the river network. Nuclide data thus support the observation of minimal alluvial sediment storage and suggest spatially uniform average erosion rates throughout the Great Smoky Mountains.

The erosion rate of the Great Smoky Mountain measured with ^{10}Be and ^{26}Al is within the range of rates calculated elsewhere in the world. Basin-wide erosion rates of tens to hundreds of meters per million years have been calculated from measured cosmogenic nuclide concentrations in various climatic and tectonic regions including very wet tropical mountains (43 mm Ky^{-1}, Brown and others, 1995), humid middle Europe (20 - 100 mm Ky^{-1}, Schaller and others, 2001), southwest United States (36 - 60 mm Ky^{-1}, Granger and others, 1996; 30 mm Ky^{-1}, Clapp and others, 2001, 2002), the Middle East (26 - 29 mm Ky^{-1}, Clapp and others, 2000), the Sierra Nevada (1.7 - 280 mm Ky^{-1}, Riebe and others, 2000), and the Oregon Coast Range (136 mm Ky^{-1}, Bierman and others, 2001; 117 mm Ky^{-1}, Heimsath and others, 2001). Far higher rates ($\sim$1000 mm Ky^{-1}) have been inferred for the Himalayas (Duncan and others, 2001; Vance and others, 2003).

Our results suggest low rates of erosion compared with other regions having significant relief and/or receiving large amounts of precipitation. The Great Smoky Mountains are eroding at rates similar to the low-relief, tectonically inactive, semi-arid granitic Llano uplift in central Texas (20 - 36 mm Ky^{-1}, Bierman and others, 2001), humid temperate middle Europe (20 - 100 mm Ky^{-1}, Schaller and others, 2001), and the crystalline rocks of the hyper-arid tectonically active southern Negev Desert in Israel (26 - 29 mm Ky^{-1}, Clapp and others, 2000). The relative low erosion rates in the stable Great Smoky Mountains support the conclusion of Riebe and others (2001a, 2001b), that base level change is the major factor controlling erosion.

Sediment Sources and Slope Transport

Distinct differences in nuclide concentration as a function of grain size allow us to infer sediment sources and understand better the sediment generation process. In the Great Smoky Mountains, smaller grain sizes yield higher ^{10}Be concentrations than larger grain sizes. The difference in cosmogenic nuclide concentration between various size grains is caused by differences in their average exposure history. Brown and others (1995) suggested that lower ^{10}Be concentrations in larger grain sizes could result from mass wasting events that excavate and carry coarse material rapidly down slope. However, there is no field evidence to indicate frequent or wide spread mass wasting events, such as debris flows, mud slides, and rockslides in our study area. Selective transport in streams would result in higher dosing of slowly transported large clasts compared with rapidly moving fine-grain material (Ferguson and others, 1996; Ferguson and Wathen, 1998). In our case, fine-grain sediment yields higher cosmogenic nuclide concentrations than large grains. Therefore, we must seek to identify a geomorphic process by which fine grains are more heavily dosed than coarse grains.

We interpret the systematic difference in nuclide concentrations, between the smaller and larger grains, as the result of the elevation distribution of their respective source areas. Material that is derived from a large elevation distribution is subjected to a higher effective production rate of cosmogenic nuclides than material that originates from a low and restricted elevation distribution. Sandstone clasts, derived from the upper parts of the slopes, break into constituent sand grains before they reach the stream due to intense chemical weathering in the soil profile (Cecil and others, 1985; Johnsson and others, 1991). Therefore, only clasts originating lower on the slopes are likely to reach the streams as coarse material before breaking into sand-size grains. We do not expect many large clasts that originate from the upper and higher parts of adjacent slopes or from further upstream to reach our sampling sites intact.

This suggestion of weathering-controlled, grain-size dependent nuclide concentration is supported by field observations. We sampled colluvium which was mostly fine-grained at the lower part of a slope in the Raven Fork basin; coarse clasts were nearly absent. In contrast, colluvium collected as sample site GSC-4, only 70 meters below the bedrock outcrop of sample GSC-3, contained many coarse fragments. The difference in coarse material content of the colluvium suggests that coarse material is most frequent nearest its bedrock source and that it rapidly breaks apart into sand-sized grains as it moves down slope.

We infer that most clasts in our large grain size fractions were derived from the lower parts of the slopes adjacent to our sampling locations. Because most clasts we sampled travel down only the lower part of the slope, they are exposed to lower effective ^{10}Be production rates and they are exposed for less time than small grains, which originated throughout, and thus on average higher, on the basin hill slopes. Consequently, coarser grains yield lower ^{10}Be concentrations (fig. 7).

If we are correct and larger clasts originate only from the lower part of the slopes adjacent to the sampling locations, then the effective basin-wide nuclide production rate does not properly describe the rate of ^{26}Al and ^{10}Be production in such clasts. Nuclide data from grain-size-specific fractions, when considered along with basin relief (ΔR), support this assertion. A positive correlation between maximum relief in the basin and the difference in normalized ^{10}Be concentrations in the different grain size fractions suggests that our explanation is valid. For example, samples taken from basins with the greatest relief (GSCO-1: ΔR ~1000 m; GSLR-7: ΔR ~1400 m) and, thus, the largest difference (ΔP) between the sampling site production rate and the effective basin-wide production rate (GSCO-1: ΔP = 37%; GSLR-7: ΔP = 34%) yielded the greatest difference in normalized ^{10}Be concentrations between the smaller and larger grain sizes. In the basin that has the smallest relief (GSCO-7; ΔR ~300 m), and the smallest difference between sampling site production rate and the effective basin-wide production rate (ΔP = 14%), ^{10}Be concentrations were similar in all grain size fractions (sample GSCO-7, fig. 7).

When ^{10}Be concentrations measured in sediments are interpreted as erosion rates using the effective basin-wide production rate, larger grain sizes yield higher model erosion rates than smaller grain sizes (fig. 7). However, to normalize accurately the measured ^{10}Be concentrations in the larger clasts requires the use of a production rate that describes the restricted and low elevation distribution from which the coarse sediment originated. It is impossible to know the exact source elevation of larger clasts and thus, to calculate the correct effective nuclide production rate for them. However, we suggest that the sampling location, a lower elevation limit for clast source in each basin, is a good proxy elevation for describing the cosmogenic nuclide production rates within the clasts. If we use such lower production rates for clasts, large grain size fractions yield erosion rates similar to those calculated from the small grain size fractions and typical for the Great Smoky Mountains (table 7, fig. 7). Such results support our assertion that clasts are derived from only the lower parts of the slopes, indicate that clasts are not transported long distances either on slopes or in rivers, and suggest that different sedimentary grain sizes are generated at similar rates in the Great Smoky Mountains. The results also indicate that nuclide concentrations in fine sand, that were measured in alluvial sediments from throughout the Great Smoky Mountains, are a reasonable proxy for basin-scale erosion rates.

Grain-size analysis results from this study and the on-slope weathering process described above are different than previous results from similar studies in arid regions. The differences in ^{10}Be concentrations among the different grain sizes were insignificant (Granger and others, 1996; Clapp and others, 2000, 2001, 2002), presumably because chemical weathering rates are far slower, where there is paucity of water and

TABLE 7

Interpretation of cosmogenic results for grain size test samples, Great Smoky Mountains

Sample name	Size fraction (μm)	^{10}Be model ε (mm Ky^{-1})	^{26}Al model ε (mm Ky^{-1})	^{10}Be Sediment generation rate (tons km^{-2} yr^{-1})[3]	^{26}Al Sediment generation rate (tons km^{-2} yr^{-1})[3]
[1]GSCO-1 (O)	250-850	28.0±3.6	29.8±4.1	76±16	80±18
[1]GSCO-1 (O)	850-2000	27.8±3.5	30.1±4.1	75±16	81±18
[2]GSCO-1 (O)	>2000	28.4±3.6	29.0±4.0	77±17	78±18
[1]GSCO-1A (O)	250-850	25.2±3.2	28.9±4.0	68±9	78±10
[1]GSCO-1A (O)	850-2000	25.5±3.3	29.9±4.3	69±9	80±11
[2]GSCO-1A (O)	2000-10000	17.8±2.3	19.7±2.8	48±6	53±8
[2]GSCO-1A (O)	>10000	29.0±3.7	27.2±3.8	78±10	73±10
[1]GSCO-7 (T)	250-850	30.5±3.9	28.3±3.9	82±18	76±17
[1]GSCO-7 (T)	850-2000	30.5±3.9	29.9±4.0	82±18	81±18
[2]GSCO-7 (T)	>2000	24.2±3.1	23.5±3.3	65±8	64±9
[1]GSLR-2 (T)	250-850	33.7±4.3	36.9±5.2	90±11	100±13
[1]GSLR-2 (T)	850-2000	37.7±4.8	41.1±5.6	101±13	111±14
[2]GSLR-2 (T)	2000-10000	37.4±4.8	35.5±4.9	101±13	96±13
[2]GSLR-2 (T)	>10000	42.7±5.5	42.6±6.0	115±15	115±13
[1]GSLR-3 (T)	250-850	49.6±6.3	N.D.	134±17	N.D.
[1]GSLR-3 (T)	850-2000	43.6±5.7	N.D.	118±15	N.D.
[2]GSLR-3 (T)	2000-10000	44.6±5.7	N.D.	120±15	N.D.
[2]GSLR-3 (T)	>10000	45.3±5.9	N.D.	122±16	N.D.
[1]GSLR-7 (O)	250-850	30.7±3.9	N.D.	83±10	N.D.
[1]GSLR-7 (O)	850-2000	30.0±3.8	N.D.	81±10	N.D.
[2]GSLR-7 (O)	2000-10000	28.5±3.6	N.D.	77±10	N.D.
[2]GSLR-7 (O)	>10000	41.5±5.3	41.8±5.7	112±14	113±15

[1]Erosion rates are calculated using basin-wide effective production rates (Bierman and Steig, 1996). [2]Erosion rates calculated using sampling site production rate (see text for discussion). [3]Sediment generation is calculated using density of 2.7 g cm^{-3}. (O)—Outlet rivers of the Great Smoky Mountains; (T)—Tributary of Oconaluftee River (GSCO) and Little River (GSLR). Erosion rates were calculated using sea-level, high-latitude ^{10}Be production rate of 5.17 atoms g^{-1} yr^{-1} supported by data from Bierman et al. (1996), Stone (2000), and Gosse and Stone (2001). ^{10}Be and ^{26}Al model ε are calculated propagating 10% (1σ) uncertainty in nuclide production rate. N.D.—no data.

thick soil mantles are rare. Thus, clasts originating throughout desert basins reach streams intact and are transported during high-energy flood events along with the fine-grain material.

Influence of Landscape Scale Parameters on ^{10}Be Concentrations and Erosion Rates

In the Great Smoky Mountains, slope gradient is the only drainage basin physical parameter that markedly correlated with basin wide erosion rates. The degree of correlation between ^{10}Be concentrations, model rates of erosion, and mean slope gradient (R^2 = 0.42, fig. 9G) indicates that colluvial processes influence the spatial pattern of erosion in the Great Smoky Mountains; alluvial processes and precipitation are less significant. As boulders and clasts break down to sand grains, the resistance of the hillslope colluvial mantle to movement decreases and sediment is transported down slope more rapidly (Mills, 2000b). As slopes steepen, the stability of the soil decreases and the rate of colluvial transport increases. This scenario shortens the residence time of the colluvium on steep slopes, relative to less steep slopes, resulting in lower cosmogenic nuclide concentrations and higher model erosion rates. In contrast to the correlation between ^{10}Be concentrations and the mean slope gradient, no correlation was found between ^{10}Be concentrations and the mean slope length in each basin. This contrast suggests that slope length is less important than slope

gradient in creating significant dosing differences, and thus ^{10}Be concentrations, in the downward moving colluvium. Indeed, the lack of correlation between ^{10}Be concentrations and slope length (fig. 9J) suggests that much of the cosmogenic nuclide accumulation occurs during bedrock weathering and not during down slope transport, a testable hypothesis.

There is a weak correlation between erosion and average elevation (fig. 9E; $R^2 = 0.22$) as well as maximum basin elevation (fig. 9A; $R^2 = 0.12$). Either correlation might result from a weak orographic effect. The orographic influence is supported by the difference in erosion rates calculated from sediments in north-flowing compared to south-flowing rivers ($p = 0.007$). Basins containing rivers that flow north from the main water divide have a higher average rate of erosion (29 ± 8 mm Ky^{-1}, $n = 17$) compared with basins containing rivers that flow south from the main drainage divide (23 ± 5 mm Ky^{-1}, $n = 26$) suggesting that differences in precipitation amounts or freeze/thaw cycles might influence erosion rates. The weak correlation ($p = 0.12$) between erosion rates and distance from the western end of the mountain range (fig. 9F), where many storms first hit, indicates that storm track does not strongly influence basin-scale erosion rates in the Great Smoky Mountains. Alluvial parameters, such as basin area (fig. 9D), relief ratio (fig. 9C), and drainage density (fig. 9H) are not significantly correlated with erosion rates.

Longitudinal profiles of the sampled rivers show knick points and convex reaches where the Thunderhead Formation sandstone caps the erodable Anakeesta Formation slates. The correlation between knick point location and convex reaches with a lithologic sequence of erodable rock capped by more resistant rock suggests the importance of lithology in determining stream profile shapes. Lithologic control is also suggested by the stability of quartz pegmatite and gneiss outcrops compared with sandstone. However, no correlation was found between basin-wide average erosion rates and the area underlain in each basin by erodable or resistant lithologies (fig. 9I).

Various drainage basin physical parameters have been examined in earlier studies attempting to understand controls on erosion rates. Summerfield and Hulton (1994) concluded that basin relief ratio is one of the most important factors controlling erosion rates whereas drainage basin area is less significant; neither appear important in the Great Smoky Mountains. Hovius (1998) and Milliman and Syvitski (1992) showed the importance of basin area and maximum basin elevation in controlling erosion rates of tectonically active mountain belts. However, Hovius (1998), Milliman and Syvitski (1992), and Pinet and Souriau (1988) show that the importance of basin area decreases dramatically when ancient orogenies (such as the Appalachian Mountains) are considered, a finding consistent with our data. Ahnert (1970) and Schumm (1963) suggested that mean basin relief is the most significant factor controlling erosion rates while precipitation was of much less importance; neither appear important in the Great Smoky Mountains. In the Himalayas, Vance and others (2003) found a significant correlation between relief and basin-wide erosion rates over three orders of magnitude of variation in erosion rate.

All these previous studies were carried out on medium to large drainage basins (generally $>10^4$ km^2) where there are considerable variations in morphology, lithology, climatic conditions, and most importantly tectonic setting within the drainage basin. For example, Hovius (1998), Milliman and Syvitski (1992), and Pinet and Souriau (1988) separated the basins they analyzed according to the level of tectonic activity and showed that the erosion rates of basins in different tectonic environments were correlated to different physical parameters. For example, they showed that in tectonically inactive areas, such as the Appalachian Mountains, the dependence of sediment yield (and by inference denudation rates) on basin area is very weak compared to high elevation and tectonically active mountain belts. The decrease in

importance of drainage area in controlling erosion rates is related to the low rates of uplift in old orogenies compared with tectonically active mountain belts. Furthermore, in many studies (for example, Summerfield and Hulton, 1994), denudation rates were based on sediment load measurements which likely do not represent the average, natural, long-term erosion rate (Meade, 1969; Milliman and Meade, 1983).

Thus, the analysis of drainage basins from various topographic and tectonic regions and which differ in size by several orders of magnitude has lead to generalizations in the importance of various drainage basin physical parameters, without recognizing that the importance of these parameters varies from one tectonic and morphologic setting to another. For example, Schaller and others (2001) show a correlation between erosion basin relief, lithology and cosmogenically estimated erosion rates in the head water channels of middle European rivers. These head water channels originate on slowly uplifted plateaus. In contrast, our study, which was conducted in a single tectonic environment with relatively minor variation in lithology and climatic conditions, does not show such correlations. We show that basin-wide erosion rates in a tectonically inactive ancient mountain belt, averaged over 10^3 - 10^5 years using cosmogenic nuclide measurements, depend mostly on basin mean slope gradient, and that other factors, such as basin area, elevation, orientation, relief, and lithology are less significant.

Implications for Large-scale Landscape Development Models of the Appalachian Mountains

Some basic concepts of geomorphology were developed in the southern and central Appalachian Mountains. In the old landscape of this mountain range, where active tectonics ceased long ago and there was no glaciation, topography has had time to adjust to lithology and structure. The *dynamic equilibrium* concept, proposed by Hack (1960), was developed in the Appalachian Mountains, where the relationship between topography, lithology, and structure could be observed. *Dynamic equilibrium* leads to the development of a steady state landscape, where relief is constant and ". . .all elements of topography are mutually adjusted so that they are down wasting at the same rate" (Hack, 1960). Our cosmogenic results and longitudinal profiles of sampled streams indicate that lithology is important in controlling the profiles of streams and slopes in the Great Smoky Mountains. However, lithology does not appear to influence rates of erosion, thus supporting Hack's assertion. Furthermore, the similarity between the average bedrock erosion rate (29 ± 13 mm Ky^{-1} for all exposed, mostly ridge top bedrock samples or 34 ± 9 mm Ky^{-1} for sandstone samples) and the basin-wide erosion rate (25 - 30 mm Ky^{-1}) suggests that the mass is being removed from all parts of the landscape at the same rate.

The *geographic cycle,* developed by Davis (1899), stemmed from his observations and ideas in the hills of Pennsylvania. Although the *geographic cycle*, as a unifying geomorphologic model, has largely been abandoned, it is interesting to note the applicability of some of its ideas to our results. The Davisian *geographic cycle* describes the change in average relief of the landscape in a way that the initial relief, after tectonic uplift ends, increases (during the youth stage) to a maximum due to deep incision by rivers. Relief then decreases as hill crests are lowered towards graded rivers. This lowering implies that slope processes are the main mechanisms of erosion during the mature and old stages of the *Geographic Cycle.* Our observations and results agree with Davis' emphasis on slope processes, specifically, the major role of slope processes in controlling the erosion rate of the Great Smoky Mountain drainage basins.

Erosion Over Time

The comparison between Cenozoic and Mesozoic erosion rates calculated from sediment yield measurements (Menard, 1961; Judson and Ritter, 1964; Gilluly, 1964; Judson, 1968; Hack, 1979; Gordon, 1979; http://webserver.cr.usgs.gov/sediment/plsql/

stateanchor; 6/01), cosmogenic nuclide analysis (this study), fission track analysis (Zimmerman, 1979; Doherty and Lyons, 1980; Naeser and others, 1999, 2001), sediment budgets (Menard, 1961), and emplacement depths of presently exposed igneous intrusions (Zen, 1991) with Paleozoic erosion rates (Pavich, 1985; Sutter and others, 1985; Zen, 1991; Huvler, 1996) suggests that high rates of denudation (>100 mm Ky^{-1}) which accompanied the Paleozoic orogenies, decreased dramatically after the termination of tectonically driven uplift.

After orogenesis ceased, low rates of erosion have apparently persisted for almost 200 My reflecting the long-term balance between erosion and rock uplift, probably driven by isostatic rebound. We are aware that variations in erosion rates have occurred (Pazzaglia and Brandon, 1996). However, we can not distinguish these variations that occurred during the time over which different techniques, including cosmogenic as well as other methodologies, average.

Our results, which describe sediment generation rates from an entire mountain range over a 10^4 - 10^5 year period, are consistent with other assessments of erosion rates through the late Cenozoic in the southern Appalachians. When extrapolated over the last 180 My, our data imply 6 to 7 kilometers of unroofing, similar to the denudation inferred from the volume of sediment deposited in the Atlantic offshore basins (Poag and Sevon, 1989). Granger and others (1997, 2001) calculated long-term ($\sim 10^6$ yr) incision rates of $\sim$30 mm Ky^{-1} for the New River (Virginia) and the Green River (Kentucky). It is possible that these long-term local incision rates are governed by the regional rate of isostatic uplift. If so, there is a striking similarity between rock uplift rate of the southern Appalachian Mountains presumably driven by erosion induced isostatic rebound and the average denudation rate we calculate in the Great Smoky Mountains.

Temporal similarity of erosion rates in the Great Smoky Mountains implies that the system may approach a state of dynamic equilibrium, when considered on time scales longer than 10^5 to 10^6 yr (Pazzaglia and Brandon, 2001; Whipple, 2001; Matmon and others, 2003), the result of steady rates of erosion persisting over 10^7 years on the spatial scale of a mountain range (Hack, 1960). The results of this study are in contrast to models that predict that initial mountain range elevation and relief are reduced by 90 percent in as little as 60 million years (Ahnert, 1970) or that complete erosion of a continent to sea level would occur within 100 to 300 My (Pinet and Souriau, 1988; Harrison, 1994). Together, a variety of data suggest the longevity of the Appalachian Mountains. Despite erosion at rates of about 30 mm Ky^{-1} for the last 180 My, the southern Appalachian Mountains still have prominent topographic expression and significant relief which might be attributed to the isostatic support of the thick crust beneath the mountain range.

CONCLUSIONS

Cosmogenic nuclide data indicate spatially homogeneous erosion of the Great Smoky Mountains at rates of 25 - 30 mm Ky^{-1}. The similarity of erosion rates calculated from ^{10}Be concentration in bedrock, alluvial sediments in headwater tributaries, and outlet rivers suggest that the entire range is being lowered at a similar rate. Cosmogenic results, field observations, and analysis of basin-scale parameters indicate the importance of slope processes in determining the spatial pattern of erosion in the Great Smoky Mountains. The data suggest that most cosmogenic nuclide accumulation occurs as bedrock weathers and as soil is transported down slope and that the rate of diffusive slope processes control sediment transport to streams draining the mountain range. Schaller and others (2001) arrived at a similar conclusion for middle Europe river systems. In the Great Smoky Mountains, alluvial and climatic factors are less significant in controlling erosion rates. Longitudinal profiles of sampled streams indicate a lithologic control over stream profile shape. However, ^{10}Be concentrations

in alluvium suggest no correlation between lithology and erosion rates, supporting Hack's (1960, 1979) basic assertion of slope adjustment to rock strength.

Cosmogenic nuclide data and field observations suggest a conceptual model for sediment generation and transport in the Great Smoky Mountains. Bedrock outcrops are rare; thus, most of the sediment in the Great Smoky Mountains must originate from the subsurface weathering of buried bedrock. The down slope movement of colluvium appears to be controlled by diffusive processes such as soil creep, tree throw, frost heaving, and bioturbation. There is little field evidence of mass wasting or surface erosion. Regression analysis of nuclide concentration and basin-scale parameters suggest that the residence time of material on the hill slopes and the down-slope movement rate of sediment are controlled by slope gradient (Gilbert, 1877; Granger and others, 1996). During down-slope transport, periods of burial that lower the $^{26}Al/^{10}Be$ ratio are not significant. Large clasts rapidly break into sand-size grains because of high weathering rates in the wet, organic-rich soils. Only clasts that originate at the lower part of the slope reach the alluvial system intact.

Sediment that reaches the river system is rapidly transported out of the mountain range. The cosmogenic data show no downstream increase in ^{10}Be concentrations within the rivers that were sampled in detail. Similar down stream cosmogenic nuclide concentration confirms the field observation of insignificant alluvial storage, indicating thorough mixing of sediment from different tributaries, and suggesting that most measured ^{10}Be is produced by cosmic-ray dosing on hill slopes rather than during fluvial transport.

Our results agree with the overall understanding of the denudational history of the Appalachians since the rifting of the Atlantic Ocean. Comparison of erosion rates, calculated by various methods in the Great Smoky Mountains and the southern Appalachians, shows that high erosion rates prevailed during the Paleozoic orogenic events that formed the Appalachians (for example, Pavich, 1985). Erosion decreased to an average and steady rate of about 30 mm Ky^{-1} which persisted over the last 180 My (for example, Naeser and others, 1999, 2001). In the Great Smoky Mountain, the relatively steady, post-orogenic erosion at a rate of ~30 mm Ky^{-1}, reflects the climatic, structural, and lithologic setting of the mountain belt and probably indicates similarity between isostatically driven uplift and denudation.

ACKNOWLEDGMENTS

Matmon supported by the U. S. Geological Survey. Analysis supported by U. S. Geological Survey and National Science Foundation grant EAR-9628599 to Bierman. Earlier versions of this paper benefited from review by the University of Vermont 2002 critical writing class. We thank T. Hanks and H. Stenner for their comments. We thank R. Single, Medical Biostatistics, University of Vermont for help with the statistical analysis, T. Kirchof and B. Wemple, Geography Department, University of Vermont, as well as C. Wentworth, and S. Brooks, U.S. Geological Survey, for help with the GIS analysis. We thank D. Granger, F. von Blanckenburg, P. Vasconcelos, and J. Garver for constructive reviews.

References

Ahnert, F., 1970, Functional relationships between denudation, relief, and uplift in large mid-latitude drainage basins: American Journal of Science, v. 268, p. 243-263.

Barron, E. J., 1989, Climate variation and the Appalachians from the late Paleozoic to the present: Results from model simulations: Geomorphology, v. 2, p. 99-118.

Beaumont, C., Kooi, H., and Willett, S., 2000, Coupled tectonic-surface process models with applications to rifted margins and collisional orogens, *in* Summerfield, M. A., editor, Geomorphology and Global Tectonics: Chichester, John Wiley, p. 29-55.

Bierman, P. R., 1994, Using in situ cosmogenic isotopes to estimate rates of landscape evolution: A review from the geomorphic perspective: Journal of Geophysical Research, v. 99, p. 13885-13896.

Bierman, P. R., and Caffee, M., 2001, Steady state rates of rock surface erosion and sediment production across the hyperarid Namib desert and the Namibian escarpment, southern Africa: American Journal of Science, v. 301, p. 326-358.

——— 2002, Cosmogenic exposure and erosion history of Australian bedrock landforms: Geological Society of America Bulletin, v. 114, n. 7, p. 787-803.

Bierman, P., and Steig, E., 1996, Estimating rates of denudation and sediment transport using cosmogenic isotope abundances in sediment: Earth Surface Processes and Landforms, v. 21, p. 125-139.

Bierman, P., and Turner, J., 1995, ^{10}Be and ^{26}Al evidence for exceptionally low rates of Australian bedrock erosion and the likely existence of pre-Pleistocene landscapes: Quaternary Research, v. 44, p. 378-382.

Bierman, P., Gillespie, A., Caffee, M., and Elmore, D., 1995, Estimating erosion rates and exposure ages with ^{36}Cl produced by neutron activation: Geochemica et Cosmochemica Acta, v. 59, p. 3779-3798.

Bierman, P., Larsen, P., Clapp, E., and Clark, D., 1996, Refining estimates of ^{10}Be and ^{26}Al production rates: Radiocarbon, v. 38, n. 1, p. 149-173.

Bierman, P. R., Marsella, K. A., Davis, P. T., Patterson, C., and Caffee, M., 1999, Mid-Pleistocene cosmogenic minimum-age limits for pre-Wisconsinan glacial surfaces in southwestern Minnesota and southern Baffin Island — a multiple nuclide approach: Geomorphology, v. 27, p. 25-40.

Bierman, P., Clapp, E. M., Nichols, K. K., Gillespie, A. R., and Caffee, M., 2001, Using cosmogenic nuclide measurements in sediments to understand background rates of erosion and sediment transport, *in* Harmon R. S., and Doe W. W., editors, Landscape erosion and evolution: New York, Kluwer/Plenum, p. 89-116.

Blackmer, G. C., Omar, G. I., and Gold, D. P., 1994, Post-Alleghenian unroofing history of the Appalachian basin, Pennsylvania, from fission track analysis and thermal models: Tectonics, v. 13, p. 1259-1276.

Boettcher, S. S., and Milliken, K. L., 1994, Mesozoic-Cenozoic unroofing of the southern Appalachian basin: apatite fission track evidence from Middle Pennsylvanian Sandstones: Journal of Geology, v. 102, p. 655-663.

Braucher, R., Brown, E. T., Bourles, D. L., and Colin, F., 2003, In-situ produced ^{10}Be measurements at great depths: implications for production rates by fast muons: Earth and Planetary Science Letters, v. 211, p. 251-258.

Brown, E., Stallard, R. F., Larsen, M. C., Raisbeck, G. M., and Yiou, F., 1995, Denudation rates determined from the accumulation of in situ-produced ^{10}Be in the Luquillo Experimental Forest, Puerto Rico: Earth and Planetary Science Letters, v. 129, p. 193-202.

Carson, M. A., and Kirkby, M. J., 1972, Hillslope form and processes: Cambridge, Cambridge University Press, 475 p.

Cecil, C. B., Stanton, R. W., Neuzil, S. G., Dulong, F. T., Ruppert, L. F., and Pierce, B. S., 1985, Paleoclimate controls on late Paleozoic sedimentation and peat formation in the central Appalachian Basin: International Journal of Coal Geology, v. 5, p. 195-230.

Clapp, E., Bierman, P. R., Schick, A. P., Lekach, Y., Enzel, Y., and Caffee, M., 2000, Sediment yield exceeds sediment production in arid region drainage basins: Geology, v. 28, p. 995-998.

Clapp E., Bierman P. R., Nichols K. K., Pavich M., and Caffee M., 2001, Rates of sediment supply to arroyos from upland erosion determined using in situ produced cosmogenic ^{10}Be and ^{26}Al: Quaternary Research, v. 55, p. 235-245.

Clapp E., Bierman P. R., and Caffee M., 2002, Using ^{10}Be and ^{26}Al to determine sediment generation rates and identify sediment source areas in an arid region drainage basin: Geomorphology, v. 45, n. 1-2, p. 67-87.

Cockburn, H. A. P., Seidl, M. A., and Summerfield, M. A., 1999, Quantifying denudation rates on inselbergs in the central Namib Desert using in situ-produced cosmogenic ^{10}Be and ^{26}Al: Geology, v. 27, p. 399-402.

Cockburn, H. A. P., Brown, R. W., Summerfield, M. A., and Seidl, M. A., 2000, Quantifying passive margin denudation and landscape development using a combined fission-track thermochronology and cosmogenic isotope analysis approach: Earth and Planetary Science Letters, v. 179, p. 429-435.

Davis, W. M., 1889, The rivers and valleys of Pennsylvania: National Geographic Magazine, v. 1, p. 183-253.

——— 1899, The geographical cycle: Journal of Geography, v. 14, p. 481-504.

Doherty, J. T., and Lyons, J. B., 1980, Mesozoic erosion rates in northern New England: Geological Society of America Bulletin, v. 91, p. 16-20.

Duncan, C. C., Masek, J. G., Bierman, P. R., Larsen, J., and Caffee, M., 2001, Extraordinarily high denudation rates suggested by ^{10}Be and ^{26}Al analysis of river sediments, Bhutan, Himalayas: Geological Society of America, Abstracts with Programs, v. 33, n. 7, p. 312.

Ferguson, R. I., and Wathen, S. J., 1998, Tracer-pebble movement along a concave river profile: Virtual velocity in relation to grain size and shear stress: Water Resources Research, v. 34, n. 8, p. 2031-2038.

Ferguson, R. I., Hoey, T., Wathen, S. J., and Werritty, A., 1996, Field evidence for rapid downstream fining of river gravels through selective transport: Geology, v. 24, n. 2, p. 179-182.

Fleming, A., Summerfield, M. A., Stone, J. O., Fifield, L. K., and Cresswell, R. G., 1999, Denudation for the southern Drakensberg escarpment, SE Africa derived from in-situ-produced cosmogenic ^{36}Cl: Initial results: London, Geological Society Journal, v. 156, p. 209-212.

Friedman, G. M., and Sanders, J. E., 1982, Time-temperature-burial significance of Devonian anthracite implies former great (~6.5 km) depth of burial of Catskill Mountains, New York: Geology, v. 10, p. 93-96.

Gilbert, G. K., 1877, Report on the geology of the Henry Mountains: U.S. Geographical and Geological Survey, 160 p.

Gilluly, J., 1964, Atlantic sediments, erosion rates, and the evolution of the continental shelf: some speculation: Geological Society of America Bulletin, v. 75, p. 483-492.

Glenn, L. C., 1926, The geology of the proposed Great Smoky Mountains National Park: Journal of the Tennessee Academy of Science, 1, n. 2, p. 13-15.
Gordon, R. B., 1979, Denudation rate of central New England determined from estuarine sedimentation: American Journal of Science, v. 279, p. 632-642.
Gosse, J. C., and Stone, J., 2001, Terrestrial cosmogenic nuclide methods passing milestones toward paleo-altimetry: American Geophysical Union, Eos, Transactions, v. 82, n. 7, p. 82, 86, 89.
Granger, D. E., and Muzikar, P. F., 2001, Dating sediment burial with in situ produced cosmogenic nuclides: theory, techniques, and limitations: Earth and Planetary Science Letters, v. 188, p. 269-281.
Granger, D. E., Kirchner, J. W., and Finkel, R., 1996, Spatially averaged long-term erosion rates measured from in-situ produced cosmogenic nuclides in alluvial sediment: Journal of Geology, v. 104, p. 249-257.
——— 1997, Quaternary down cutting rate of the New River, Virginia measured from differential decay of cosmogenic ^{26}Al and ^{10}Be in cave-deposited alluvium: Geology, v. 25, p. 107-110.
Granger, D. E., Fabel, D., and Palmer, A. N., 2001, Pliocene-Pleistocene incision of the Green River, Kentucky, determined from radioactive decay of cosmogenic ^{26}Al and ^{10}Be in Mammoth Cave sediments: Geological Society of America Bulletin, v. 113, n. 7, p. 825-836.
Hack, J. T., 1960, Interpretation of erosional topography in humid temperate regions: American Journal of Science, v. 258-A, p. 80-97.
——— 1979, Rock control and tectonism, their importance in shaping the Appalachian highlands: U.S. Geological Survey Professional Paper, v. 1126-B, p. 17.
——— 1982, Physiographic divisions and differential uplift in the Piedmont and Blue ridge: U. S. Geological Survey Professional Paper 1265, 49 p.
Hadley, J. B., and Goldsmith, R., 1963, Geology of the eastern Great Smoky Mountains, North Carolina and Tennessee: U. S. Geological Survey professional paper 349-B, 118 p.
Hamilton, W. B., 1961, Geology of the Richardson Cove and Jones Cove quadrangles, Tennessee: U. S. Geological Survey professional paper 349-A, 55 p.
Harrison, C. G. A., 1994, Rates of continental erosion and mountain building: Geologische Rundschau, v. 83, n. 2, p. 431-447.
Heimsath, A. M., Dietrich, W. E., Nishiizumi, K., and Finkel, R. C., 1997, The soil production function and landscape equilibrium: Nature, v. 388, n. 6640, p. 358-361.
——— 1999, Cosmogenic nuclides, topography, and the spatial variation of soil depth: Geomorphology, v. 27, p. 151-172.
Heimsath, A. M., Chappell, J., Dietrich, W. E., Nishiizumi, K., and Finkel, R. C., 2000, Soil production on a retreating escarpment in southeastern Australia: Geology, v. 28, n. 9, p. 787-790.
Heimsath, A. M., Dietrich, W. E., Nishiizumi, K., Finkel, R. C., 2001, Stochastic processes of soil production and transport: erosion rates, topographic variation and cosmogenic nuclides in the Oregon Coast Range: Earth Surface Processes and Landforms, v. 26, p. 531-552.
Heimsath, A. M., Chappell, J., Spooner, N. A., and Questiaux, D. G., 2002, Creeping soil: Geology, v. 30, n. 2, p. 111-114.
Hovius, N., 1998, Controls on sediment supply by large rivers, *in* Shanley, K. W., and McCabe, P. J., editors, Relative role of eustasy, climate, and tectonism in continental rocks: Society for Sedimentary Geology Special Publication, v. 59, p. 3-16.
Hutchinson, D. R., Grow, J. A., and Klitgord, K. D., 1983, Crustal structure beneath the southern Appalachians: non-uniqueness of gravity modeling: Geology, v. 11, p. 611-615.
Huvler, M. L., 1996, Post-orogenic denudation and mass-balanced topography of the Appalachian Mountain system from maturation indicators, thermochronology, and metamorphic petrology: Geological Society of America, Abstracts with Programs, v. 28, n. 7, p. 500.
Iverson, W. P., and Smithson, S. B., 1983, Reprocessing and reinterpretation of COCORP southern Appalachian profiles: Earth and Planetary Science Letters, v. 62, p. 75-90.
Jennings, K., Bierman, P., and Southon, J., 2003, Timing and style of deposition on humid-temperate fans, Vermont, U.S.A.: Geological Society of America Bulletin, v. 115, n. 2, p. 182-199.
Johnsson, M. J., Stallard, R. F., and Lundberg, N., 1991, Controls on the composition of fluvial sands from a tropical weathering environment: Sands of the Orinoco River drainage basin, Venezuela and Colombia: Geological Society of America Bulletin, v. 103, p. 1622-1647.
Judson, S., 1968, Erosion of the land or what's happening to our continents: American Scientist, v. 56, p. 356-374.
——— 1975, Evolution of the Appalachian topography, *in* Melhorn, W. N., and Flemal, R. C., editors, Theories of landform development: Binghamton, New York, Publications in Geomorphology, p. 29-44.
Judson, S., and Ritter, D., 1964, Rates of regional denudation in the United States: Journal of Geophysical Research, v. 69, p. 3395-3401.
Keith, A., 1895, Description of the Knoxville sheet (Tennessee-North Carolina): U.S. Geological Survey, Geological Atlas, Folio 16, 6 p.
King, P. B., 1964, Geology of the central Great Smoky Mountains, Tennessee: U. S. Geological Survey Professional Paper, p. 1-148.
King, P. B., Neuman, R. B., and Hadley, J. B., 1968, Geology of the Great Smoky Mountains National Park, Tennessee and North Carolina: U. S. Geological Survey Professional Paper 587, 23 p.
Kirchner, J. W., Finkel, R. C., Riebe, C. S., Granger, D. E., Clayton, J. L., King, J. G., and Megahan, W. F., 2001, Mountain erosion over 10 yr., 10 Ky and 10 My time scales: Geology, v. 29, n. 7, p. 591-594.

Klein, J., Giegengack, R., Middleton, R., Sharma, P., Underwood, J. R., Jr., and Weeks, R. A., 1986, Revealing histories of exposure using in situ produced ^{26}Al and ^{10}Be in Libyan Glass: Radiocarbon, v. 28, p. 547-555.

Kochel, R. C., 1990, Humid fans of the Appalachian Mountains, *in* Rachocki, A. H., and Church, M., editors, Alluvial Fans, A Field Approach: Chichester, United Kingdom, John Wiley and Sons, p. 109-129.

Lal, D., 1988, In situ-produced cosmogenic isotopes in terrestrial rocks: Annual Reviews of Earth and Planetary Science, v. 16, p. 355-388.

——— 1991, Cosmic ray labeling of erosion surfaces: *In situ* production rates and erosion models: Earth and Planetary Science Letters, v. 104, p. 424-439.

Lal, D., and Arnold, J. R., 1985, Tracing quartz through the environment: Earth and Planetary Science, Proceedings of the Indian Academy of Science, v. 94, p. 1-5.

Matmon, A., Bierman, P., Larsen, J., Southworth, S., Pavich, M., and Caffee, M., 2003, Temporally and spatially uniform rates of erosion in the southern Appalachian Mountains: Geology, v. 31, n. 2, p. 155-158.

Meade, R. H., 1969, Errors in using modern stream load data to estimate natural rates of denudation: Geological Society of America Bulletin, v. 80, p. 1265-1274.

Menard, H. W., 1961, Some rates of regional erosion: Journal of Geology, v. 69, p. 154-161.

Milliman, J. D., and Meade, R. H., 1983, Worldwide delivery of river sediment to the oceans: Journal of Geology, v. 91, p. 1-21.

Milliman, J. D., and Syvitski, P. M., 1992, Geomorphic/tectonic control of sediment discharge to the ocean: The importance of small mountainous rivers: The Journal of Geology, v. 100, p. 525-544.

Mills, H. H., 2000a, Apparent increasing rates of stream incision in the Eastern United States during the late Cenozoic: Geology, v. 28, p. 955-957.

——— 2000b, The relationship of slope angle to regolith clast size; a test of dynamic equilibrium based on surficial mapping in the southern Blue Ridge, North Carolina: Southeastern Geology, v. 39, n. 3-4, p. 243-258.

Mills, H. H., Brakenridge, G. R., Jacobson, R. B., Newell, W. I., Pavich, M. J., and Pomeroy, J. S., 1987, Appalachian Mountains and plateaus, *in* Graf, W. L., editor, Geomorphic Systems of North America: Geological Society of America, Centennial Special Volume n. 2, p. 5-50.

Naeser, C. W., Naeser, N. D., Kunk. M. J., Morgan, B. A., III, Schultz, A. P., Southworth, C. S., and Weems, R. E., 2001, Paleozoic through Cenozoic uplift, erosion, stream capture, and deposition history in the Valley and Ridge, Blue Ridge, Piedmont, and Coastal Plain province of Tennessee, North Carolina, Virginia, Maryland, and District of Columbia: Geological Society of America, annual meeting, Abstracts with Programs, v. 33, n. 6, p. 312.

Naeser, N. D., Naeser, C. W., Morgan, B. A., III, Schultz, A. P., and Southworth, C. S., 1999, Paleozoic to Recent cooling history of the Blue Ridge Province, Virginia, North Carolina, and Tennessee, from apatite and zircon fission-track analysis: Geological Society of America, annual meeting, Abstracts with Programs, v. 31, n. 7, p. 117.

Nishiizumi, K., Lal, D., Klein, J., Middleton, R., and Arnold, J. R., 1986, Production of ^{10}Be and ^{26}Al by cosmic rays in terrestrial quartz *in situ* and implications for erosion rates: Nature, v. 319, p. 134-136.

Nishiizumi, K., Winterer, E. L., Kohl, C. P., Klein, J., Middleton, R., Lal, D., and Arnold, J. R., 1989, Cosmic ray production rates of ^{10}Be and ^{26}Al in quartz from glacially polished rocks: Journal of Geophysical Research, v. 94, p. 17907-17915.

Nishiizumi, K., Kohl, C. P., Arnold, J. R., Klein, J., Fink, D., and Middleton, R., 1991, Cosmic ray production rates of ^{10}Be and ^{26}Al in Antarctic rocks: exposure and erosion history: Earth and Planetary Science Letters, v. 104, p. 440-454.

Nott, J., and Roberts, R. G., 1996, Time and process rates over the last 100 my: a case for dramatically increased landscape denudation rates during the late Quaternary in northern Australia: Geology, v. 24, p. 883-887.

Pavich, M. J., 1985, Appalachian Piedmont morphogenesis: weathering, erosion and Cenozoic uplift, *in* Morisawa, M., and Hack, J. T., editors, Tectonic Geomorphology, Proceedings of the 15th annual Binghamton geomorphology symposium: Boston, Unwin Hyman, p. 299-319.

Pazzaglia, F. J., and Brandon, M. T., 1996, Macrogeomorphic evolution of the post-Triassic Appalachian Mountains determined by deconvolution of the offshore basin sedimentary record: Basin Research, v. 8, p. 255-278.

——— 2001, A fluvial record of long-term steady-state uplift and erosion across the Cascadia forearc high, western Washington State: American Journal of Science, v. 301, p. 385-431.

Pazzaglia, F. J., and Gardner, T. W., 2000, Late Cenozoic landscape evolution of the US Atlantic passive margin: insights into a North American Great Escarpment, *in* Summerfield, M. A., editor, Geomorphology and Global Tectonics: Chichester, John Wiley, p. 283-303.

Pinet, P., and Souriau, M., 1988, Continental erosion and large-scale relief: Tectonics, v. 7, n. 3, p. 563-582.

Poag, C. W., and Sevon, W. D., 1989, A record of Appalachian denudation in postrift Mesozoic and Cenozoic sedimentary deposits of the U. S. middle Atlantic continental margin: Geomorphology, v. 2, p. 119-157.

Riebe, C. S., Kirchner, J. W., Granger, D. E., and Finkel, R. C., 2000, Erosional equilibrium and disequilibrium in the Sierra Nevada, inferred from cosmogenic ^{26}Al and ^{10}Be in alluvial sediments: Geology, v. 28, n. 9, p. 803-806.

——— 2001a, Minimal climatic control on erosion rates in the Sierra Nevada, California: Geology, v. 29, n. 5, p. 447-450.

——— 2001b, Strong tectonic and weak climatic control of long-term chemical weathering rates: Geology, v. 29, n. 6, p. 511-514.

Roden, M. K., and Miller, D. S., 1989, Apatite fission-track thermochronology of the Pennsylvania Appalachian basin: Geomorphology, v. 2, p. 39-51.

Schaller, M., von Blanckenburg, F., Hovius, N., and Kubik, P. W., 2001, Large scale erosion rates form in situ-produced cosmogenic nuclides in European river sediments: Earth and Planetary Science Letters, v. 188, p. 441-458.

Schultz, A., and Southworth, S., 1999, Geologic history and geologic map of Great Smoky Mountains National Park: Gatlinburg, Tennessee, Great Smoky Mountains Natural History Association.

Schultz, A., Southworth, S., Fingeret, C., and Weik, T., 2000, Digital geologic map and WEB site of the Mount LeConte 7.5-minute quadrangle, Great Smoky Mountains National Park, Tennessee and North Carolina: U. S. Geological Survey, Open-File Report 00-261.

Schumm, S. A., 1963, The disparity between present rates of denudation and orogeny: U. S. Geological Survey Professional Paper, 454-H, 13 p.

Slingerland, R., and Furlong, K. P., 1989, Geodynamic and geomorphic evolution of the Permo-Triassic Appalachian Mountains: Geomorphology, v. 2, p. 23-37.

Small, E. E., Anderson, R. S., and Hancock, G. S., 1999, Estimates of the rate of regolith production using ^{10}Be and ^{26}Al from an alpine hillslope: Geomorphology, v. 27, p. 131-150.

Southworth, S., 1995, Preliminary geologic map of the Great Smoky Mountains National Park within the Fontana Dam and Tuskeegee quadrangles, Swain County, North Carolina: U. S. Geological Survey Open-File Report 95-264, scale-1:24,000, 33 p.

——— 2001, The Link between Geology, GIS, and ATBI Plots, Gatlinburg, Tennessee: ATBI Quarterly Spring Newsletter, Discover Life in America, p. 6-7.

Southworth, S., Chirico, P., and Putbrese, T., 1999, Digital geologic map of parts of the Cades Cove and Calderwood quadrangles, Tennessee and North Carolina, Great Smoky Mountains National Park: U. S. Geological Survey Open-File Report 99-175, scale 1:24,000

Southworth, S., Schultz, A., Denenny, D., and Triplett, J., 2003, Preliminary Surficial Geologic Map of the Great Smoky Mountains National Park Region, Tennessee and North Carolina: U. S. Geological Survey Open File Report 03-381, 1:1000,000-scale.

Stone, J., 2000, Air pressure and cosmogenic isotope production: Journal of Geophysical Research, v. 105, n. B10, p. 23753-23759.

Summerfield M. A., and Hulton, N. J., 1994, Natural controls of fluvial denudation rates in major world drainage basins: Journal of Geophysical Research, v. 99, n. B7, p. 13871-13883

Summerfield, M. A., Sugden, D. E., Denton, G. H., Marchant, D. R., Cockburn, H. A. P., and Stuart, F. M., 1999, Cosmogenic isotope data support previous evidence of extremely low rates of denudation in the Dry Valley region, southern Victoria Land, Antarctica, *in* Smith, B. J., Whalley, W. B., and Warke, P. A., editors, Uplift, erosion and stability; perspectives on long-term landscape development: London, Geological Society of London, Geological Society Special Publications 162, p. 255-267.

Sutter, J. F., Ratcliffe, N. M., and Musaka, S. B., 1985, ^{40}Ar/^{39}Ar and K-Ar data bearing on the metamorphic and tectonic history of western New England: Geological Society of America Bulletin, v. 96, p. 123-136

Tucker, G. E., and Slingerland, R. L., 1994, Erosional dynamics, flexural isostasy, and long-lived escarpments: A numerical modeling study: Journal of Geophysical Research, v. 99, p. 12,229-12,243.

Vance, D., Bickle, M., Ivy-Ochs, S., Kubik, P. W., 2003, Erosion and exhumation in the Himalaya from cosmogenic isotope inventories of river sediments: Earth and Planetary Science Letters, v. 206, p. 273-288.

Whipple, K. X., 2001, Fluvial landscape response time; how plausible is steady state denudation?: American Journal of Science, v. 301, n. 4-5, p. 313-325.

Zen, E., 1991, Phanerozoic denudation history of the southern New England Appalachians deduced from pressure data: American Journal of Science, v. 291, p. 401-424.

Zimmerman, R. A., 1979, Apatite fission track age evidence of post-Triassic uplift in the central and southern Appalachians: Geological Society of America Abstracts with Programs, v. 11, p. 219.